

Use of the blocking effect to measure nuclear reaction times

S. A. Karamyan, Yu. V. Melikov, and A. F. Tulinov

Joint Institute for Nuclear Research, Dubna

M. V. Lomonosov Moscow State University

Fiz. EL. Chast. Atom. Yad., 4, 456-511 (April-June 1973)

Literature on the use of the blocking effect to measure nuclear reaction times is reviewed. The physical nature of the orientational effects which arise as charged particles move through a crystal is analyzed. There is a brief review of the theory of the blocking effect and of the basic principles of measuring the nuclear lifetimes in the range $\tau < 10^{-15}$ sec. The various types of experiments which have been carried out and the various methods which have been used to extract lifetimes from the experimental data are discussed. There is a summary of the results found in measurements of lifetimes of compound nuclei in inelastic scattering of protons, in (p, α) reactions, and in the fission of heavy nuclei by neutrons, protons, and heavy ions. The experimental results are compared with results calculated on the basis of the statistical model of the compound nucleus.

INTRODUCTION

A remarkable feature of nuclear reactions is that the characteristic times involved span the entire range of time intervals which can be determined physically. The half-lives of heavy nuclei with respect to spontaneous fission (10^{15} – 10^{20} yr) are known to exceed the ages of all known astronomical objects; at the other end of the time scale, certain nuclear reactions occur within the shortest time interval which arises in physics: $t_{\min} \sim 10^{-24}$ sec, determined from the ratio $t_{\min} = r_{\min}/c$, where r_{\min} is the size of the nucleon and c is the speed of light. The characteristic time for a nuclear reaction is usually governed by the mean lifetime τ of the corresponding unstable nuclear system. This time refers to characteristics of nuclear states which are not quantized, so it is particularly sensitive to structural details; although essentially no use has yet been made of this high sensitivity, it will undoubtedly increase in importance as our understanding of nuclear phenomena improves.

Except for such slow nuclear reactions as radioactive decay, the study of the lifetimes of nuclear states has always been and still is accompanied by the invention of special methods for measuring even shorter time intervals. This increasing sophistication of experimental techniques allows experimenters to continually extend their study to higher-lying nuclear excitations.

At present, essentially the entire range of excited states below the threshold for nucleon emission has been studied. In this range the excitation decays through an electromagnetic transition, for which the characteristic time is $\sim 10^{-9}$ – 10^{-15} sec. A great variety of experimental methods have been developed for this time range; the most common are based on the use of delayed coincidence, the Doppler effect, Coulomb excitation of nuclei, and resonance scattering of γ 's. Through the use of these and other methods experimentalists have now accumulated a huge store of information on τ values; this information has been used primarily to develop and refine various nuclear models.

The situation is entirely different in the range of excitations having energies above the energy for nuclear dissociation. Here the probability for the decay of a state increases sharply because nucleon channels become available, decay of a state increases sharply because nucleon channels become available and the lifetime of the state drops accordingly. This situation is characteristic for

nuclear reactions induced by nucleons. The lifetime of the compound system formed by the incident particle and the target nucleus is governed by the structure of the compound nucleus and the reaction mechanism; at present this lifetime cannot be predicted theoretically. There are certain limiting cases, however, in which the characteristic times for nuclear reactions can be estimated: in direct reactions, for which the characteristic times are on the order of 10^{-22} – 10^{-23} sec, and in reactions in which a compound nucleus forms in 10^{-15} – 10^{-20} sec, as a result of the energy distribution among a large number of nucleons. Until recently no direct methods were available for measuring time intervals in this range, i.e., no methods were available which were based on a comparison of the nuclear reaction time with the characteristic time of some other, sufficiently well understood physical process. The problem of finding such a method has been extremely complicated, and the solution of this problem has only just begun. The method reviewed below represents an important step in this solution. Before we turn to this method, however, we will review certain questions which arise in the use of indirect methods to determine τ which are based on measurement of the widths Γ of nuclear states.

The value of Γ can be determined most naturally for isolated resonance reactions. Here the widths are determined either by direct measurement involving excitation functions or by measuring the yields of the corresponding resonance reactions. Unfortunately, this possibility is only open for an extremely narrow range of nuclear-excitation energies, slightly above the dissociation threshold. At higher excitation energies of the compound nucleus the level spacing D becomes comparable to the width Γ because of increases in both the level density and level width. Here it is essentially impossible to observe resonances corresponding to individual levels, so it is essentially impossible to determine the level widths directly. At higher excitation energies, however, at which the levels of the compound nucleus overlap significantly, an indirect method based on study of the fluctuations in the effective cross sections for nuclear reactions can be used to measure widths. Because of the strong interest in this method, we will discuss its physical nature and the outlook for its use. The fluctuation method was developed by Ericson¹⁻⁵ for the case $\Gamma \gg D$.

The idea behind this method can be outlined in the following manner: We assume that a compound nucleus forms through an interaction of a monoenergetic particle beam of energy E_0 with the target nucleus. Then for $\Gamma \gg D$ we

find the simultaneous excitation of many states lying in an energy range on the order of $\bar{\Gamma}$, where $\bar{\Gamma}$ is the level width averaged over some range of excitation energies. The reaction amplitude is the sum of the amplitudes corresponding to the various excited states. If there is a sufficient number of these states, we can assume the phases of the various levels to be mutually independent and capable of taking on all possible values. By statistically combining the amplitudes we can then find any reaction cross section, down to a vanishing cross section. When the energy of the incident particles is changed by an amount $\delta E_0 > \bar{\Gamma}$, a different set of levels is excited. Now the complete set of phase shifts is different, statistically independent of the previous set, so the cross section assumes a completely different value. If the energy values differ by $\delta E_0 < \bar{\Gamma}$, it is largely the same group of levels which are excited. The appreciable correlation between the sets of phase shift smoothes the cross section.

Accordingly, by exploiting the continuity of the cross section as a function of the energy, using correlation analysis to analyze this cross section, we can extract the value of $\bar{\Gamma}$, which in this case has the meaning of a coherence interval.³ In the Ericson fluctuation theory this quantity is called the "coherence width." It is important to note that where the levels overlap significantly, the quantity $\bar{\Gamma}$ is not the level width in the Breit-Wigner sense, but instead represents a mean nuclear lifetime τ for the given excitation energy.⁶

Several factors tend to reduce the fluctuations, and some of them set a limit on the applicability of this method for measuring the lifetimes of compound nuclei. One factor is the presence of a direct-interaction mechanism in the reaction being studied: The greater the contribution of the direct mechanism to the reaction amplitude, the weaker the fluctuation in the cross section. Any averaging or summation of amplitudes for cross sections tends to reduce the fluctuations. This reduction is observed, e.g., when the cross section is found by summing over different orientations of the spins and orbital angular momenta of the nuclei involved in the reaction or when the nuclear excitation energy becomes so high that too many overlapping states are involved. An increase in the number of final states corresponding to the cross section being measured has the same effect. Accordingly, we say that reactions forming a definite level in the product nucleus have a much higher fluctuation amplitude than those for which the measured cross sections are integrated over angular or energy ranges. Finally, Ericson fluctuations are very sensitive to an increase in the energy spread in the incident beam. If this spread, ΔE_0 , exceeds $\bar{\Gamma}$, the fluctuation range falls off by a factor of $\sim \sqrt{\Delta E_0 / \bar{\Gamma}}$. Since the minimum energy spread in the incident beam may be on the order of ~ 1 keV, we find under the condition $\Delta E_0 \ll \bar{\Gamma}$ that the lower limit on the measurable coherence width is about 10 keV. Adopting the nuclear-excitation range of 15-25 MeV as the most convenient experimentally, we find that the value $\bar{\Gamma} \sim 10$ keV limits the applicability of this method to compound nuclei having mass numbers $A \leq 40$.

Many experimental studies of cross-section fluctuations for these nuclei have been reported (see, e.g., the bibliography in ref. 5). The measured lifetimes have

turned out to lie in the range $5 \cdot 10^{-20}$ - $5 \cdot 10^{-21}$ sec. Transition to the range $A > 40$ without a significant reduction of the energy spread in the incident beam violates the condition $\Delta E_0 \ll \bar{\Gamma}$ and thus complicates the determination of τ . In recent years, however, attempts have been made to extend the fluctuation method to the range of slightly heavier nuclei having much smaller coherence widths for this excitation-energy range. Here the condition $\Delta E_0 > \bar{\Gamma}$ is satisfied. It turns out that if we incorporate in the correlation functions certain corrections taking into account fluctuation damping⁷ we can, in principle, evaluate $\bar{\Gamma}$ for nuclei in the range $A \leq 100$. This is an interesting possibility since it extends the range of measurable times⁸ to $5 \cdot 10^{-18}$ sec, but the results found under these conditions suffer from very large statistical errors, which increase with increasing A .

While acknowledging the importance of measurements of nuclear reaction times through an analysis of cross-section fluctuations, we must note that there are fundamental difficulties involved in interpreting the corresponding results: To calculate the coherence width we must use a specific form of the dependences of the scattering amplitudes for the various levels on the energy, angular momentum, etc., but these dependences are not known in the range of overlapping levels. The approximations which have been used are extremely arbitrary. It thus becomes extremely desirable to compare the results found by this indirect method with the results found from more direct measurements of τ . Since the method described below is at present the only direct method available, this future comparison will evidently be based on this method.

The method with which we are concerned here is that based on the blocking effect. This effect refers to a number of so-called orientational effects which arise in the interaction of fast charged particles with crystals. It is closely related to another effect in the same category, customarily called the channeling effect. These two effects involve two groups of particles moving in a crystal under extremely different conditions: Channeling involves particles whose trajectories lie in "voids" of the crystal, while blocking involves particles moving in the maximum-density parts of the crystal. The channeling effect was the first discovered in a study of the dependence of the range of charged particles in a crystal on the orientation of the crystal with respect to the incident beam.⁹

It was found that many of the particles moving along the main crystallographic axes have unusually long ranges. Further study showed the range increase to be one aspect of the overall behavior observed as particles are incident at a small angle on an ordered array of nuclei. The particles are reflected from the array as a whole and may retain their longitudinal motion for a long time, remaining relatively far from regions dense in nuclear matter.

This particle motion, described in detail in the classical study by Lindhard,¹⁰ has several consequences. First, the specific energy loss due to electron collisions which is suffered by particles moving under channeling conditions should be quite low, since the electron density near the channel axis is much lower than the average electron density in the medium. Second, the probability for nuclear

reactions involving these particles is low, since the channeled particles move in trajectories far from the nuclei. Channeling has been detected in the motion of particles along crystal planes as well as along axes. Significantly, for both axial and planar channeling the requirement that the angle between the crystallographic direction and the particle trajectory be small means that the effect can be observed in its relatively pure form only when particles are injected into a crystal.

The situation is different if the particles come from lattice sites in the crystal. In this case the charged particles emitted parallel to crystallographic axes and planes are significantly scattered by the nearest nuclei, so their trajectories deviate from the initial direction. Accordingly, the directions corresponding to the crystallographic axes and the planes are blocked for these particles; because of the translational symmetry of the lattice, all these directions are blocked, regardless of the positions of the sites from which the particles are emitted.

Accordingly, the angular distributions of particles escaping from the crystal display "dips," or regions of sharply reduced intensity, whose nature is governed by the crystal structure. The blocking effect was discovered simultaneously and independently in two different types of experiments. In one, α particles were emitted from lattice sites as a result of radioactive decay,¹¹ while in the other reaction products were emitted.¹²⁻¹⁴ Reports^{12,13} of the observation of the blocking effect were accompanied by discussions of the possible uses of this effect to experimentally determine nuclear reaction times. The idea behind this method can be described as follows: A study is made of a nuclear reaction in a crystal. During the reaction, a compound nucleus is moved from its lattice site by the momentum of the incident particle. When a particle—a reaction product—is emitted, the compound nucleus lies on the average at a distance of $s = v\tau$ from its lattice site, where v is the velocity of the compound system and τ is its mean lifetime. The displacement of the source from the site affects the shape of the dip in the angular distribution of reaction products; the most important component of this recoil distance is obviously that normal to the crystallographic axis or plane (Fig. 1).

We can immediately draw some very general conclusions about the range of compound-nucleus lifetime measurable by this method. We start from the fact that the recoil of the compound nucleus from the lattice site significantly affects the dip shape only if the normal component of this recoil is comparable to the distance over which the atomic-electron field screening the nucleus begins to become important. We thus find $5 \cdot 10^{-10}$ cm <

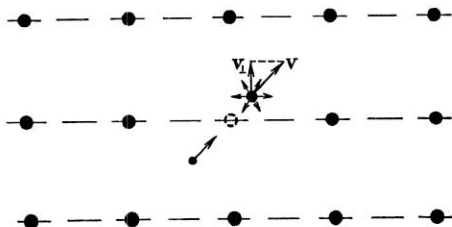


Fig. 1. Recoil of a compound nuclear system from a lattice site caused by momentum transfer from an incident particle.

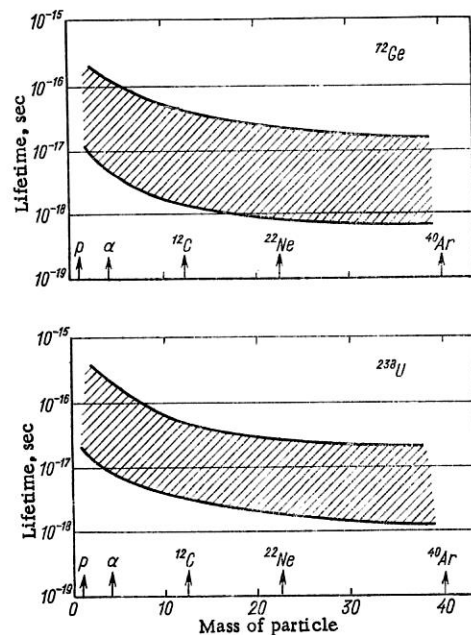


Fig. 2. Lifetime range of excited compound nuclei measurable by the blocking effect during bombardment of germanium and uranium nuclei by charged particles.

$v_1\tau \lesssim 10^{-8}$ cm, where the upper limit is governed by the lattice constant. We see that the range of times measurable depends strongly on the velocity acquired by the compound nucleus, i.e., ultimately, on the energy of the particles in the primary beam and on the masses of the nuclei involved. Figure 2 shows the calculated range of measurable τ values for the compound nuclei produced from a nucleus of medium mass (^{72}Ge is adopted here as an example) and from a heavy nucleus (^{238}U) when these nuclei are bombarded by various accelerated charged particles. The energy of the incident particles is assumed equal to the Coulomb fusion barrier. We see that in principle this method can be used to measure lifetimes in the range 10^{-15} – 10^{-18} sec, a range of much interest in the physics of nuclear reactions. Furthermore, as we will see from the discussion below, the outlook is promising for extension of the blocking method to even smaller values of τ . Taking into account the tendency mentioned above for an increase in the upper limit on times measurable by the fluctuation method, we see that it will become possible to compare the results obtained by the two methods.

To conclude this introduction we note that it was mentioned above that the initial step in the development of this new method for measuring τ was the experimental discovery of the blocking effect. However, it turned out that a group of physicists at an Australian university came very close to developing this new method several years earlier. Unfortunately, the preliminary experiments carried out by this group were unsuccessful, and the study was not pursued.

THE BLOCKING EFFECT AND SOME ASSOCIATED BEHAVIOR

Here we are concerned with those aspects of the physics of the blocking effect which are pertinent to a determination of τ . In general, of course, the interaction of

particles with a crystal must be analyzed by the methods of quantum mechanics. This approach has been used^{15,16} to describe orientational effects; it was found that under certain conditions purely quantum effects should be taken into account, but in essentially all cases of interest in connection with our method of determining τ the blocking effect can be described on the basis of classical ideas.

The classical approach simplifies the analysis of the formation of the blocking pattern, in particular, because in the classical approach the formation of the pattern observed experimentally can be divided into two successive steps.

The first step is the formation of that pattern which is conveniently called the "primary pattern," i.e., that minimum which would be found in the angular distribution of particles emitted from lattice sites if the distribution were recorded immediately after the particles escaped the axes or planes from which they were emitted. In other words, the primary pattern is that produced by a single axis or a single plane.

Since in an actual experiment particles are emitted from sites which are generally at some depth in the interior of a crystal, there is an unavoidable second step: the change in the primary pattern due to interactions of the emitted particles with other axes or planes. These interactions, which continue until the particles escape from the crystal, convert the primary pattern into that which is detected experimentally.

This division of the effect into two steps of course brings us little closer to a systematic solution of the problem of finding a theoretical description of the pattern shape and of the effect on this shape of the displacement of the compound nucleus from the lattice site. At present there is no satisfactory theory for either step. On the other hand, this division does allow us to use various highly simplified models. We turn now to a slightly more detailed discussion of the formation of the primary pattern, first an axial pattern and then a planar one.

It is convenient to adopt the following model in analysis of the primary axial pattern: There is an infinitely long chain with vibrating atoms. The deviations of these atoms from their equilibrium positions are described by some distribution, e.g., Gaussian. The vibrations are assumed isotropic and uncorrelated. The vibration amplitude is related to the temperature; this is done most easily by using the Debye model. Charged particles are emitted from nuclei of this chain in some primary angular distribution with respect to the chain axis. In certain cases this distribution can be assumed isotropic.

The interaction of the particles with the individual atoms of the chain is described by the Thomas-Fermi potential, which is frequently approximated by the familiar Moliere equation¹⁷ or Lindhard equation.¹⁰ Under these assumptions the blocking pattern observed at a small angle with respect to the chain axis will obviously be axially symmetric, having a minimum at the axis and an annular "shoulder" lying at some angle with respect to the axis. Despite the simplicity of this picture, no analytic expression has yet been obtained for the shape of the primary axial pattern. On the other hand, much information has been obtained from Monte Carlo computer calculations of

the shapes of such patterns (see, e.g., ref. 18). These results furnish a basis not only for studying the dependences of the pattern shape on various parameters (the charge of the chain nuclei, that of the emitted particles, the particle energy, the amplitude of the atomic vibrations, and the spacing of atoms in the chain, but also for checking the accuracy of analytic calculations.

A few attempts have been made to obtain analytic expressions; although they do not describe the entire angular distribution, they do allow calculations of certain pattern parameters. Two parameters turn out to be the most useful: the ratio χ of the particle intensity at the center of the dip to that far from the dip, and the dip width, e.g., at the half-maximum level. The width is frequently characterized by the angle ψ , half the total width.

The first analytic evaluation¹² of the angle ψ for a vibrating chain was based on the following assumptions: The chain atoms are a set of independent three-dimensional classical oscillators in oscillation with an amplitude u . The interaction of a particle emitted from a site with the chain atoms is described by the familiar Bohr potential

$$V = (Z_1 Z_2 e^2 / r) \exp(-r/a),$$

where $Z_1 e$ and $Z_2 e$ are the charges of the emitted particle and the scattering nuclei, respectively, and a is the screening parameter. As the particles move within the cylindrical region of radius u around the chain, they undergo ordinary multiple scattering; outside this region they are acted on by the decaying average field of the chain atoms. These assumptions lead to

$$\psi^2 = \left[\frac{3}{2} \cdot \frac{b^2}{ul} \ln \frac{a}{b} \right]^{2/3} + 2 \frac{b}{l} K_0 \left(\frac{u}{a} \right), \quad (1)$$

where $b = Z_1 Z_2 e^2 / E$, l is the distance between neighboring atoms in the chain, $K_0(x)$ is the modified Hankel function, and E is the energy of the moving particle.

Despite the crude assumptions used in the derivation of Eq. (1), further study showed that this equation gives a qualitatively correct dependence of ψ on various factors, in particular, the temperature.¹⁴ A completely different approach was used in refs. 10 and 19 to determine the dip parameters. This approach is based on the "string" potential found by averaging the potential of a rigid discrete chain along its axis; the string potential is

$$U(r) = (Z_1 Z_2 e^2 / l) \ln [(Ca/r)^2 + 1]. \quad (2)$$

This potential is quite reliable for describing channeling effects, since the discrete nature of the actual chains is largely suppressed as the particles move near the channel axis. Analytically, this potential represents an important simplification, since it reduces the problem essentially to the solution of a purely potential problem. In this problem the complicated particle trajectory is characterized by the single variable E_\perp , the total energy associated with the transverse motion:

$$E_\perp = U(r) + E\varphi^2, \quad (3)$$

where φ is the instantaneous angle between the particle trajectory and the chain axis.

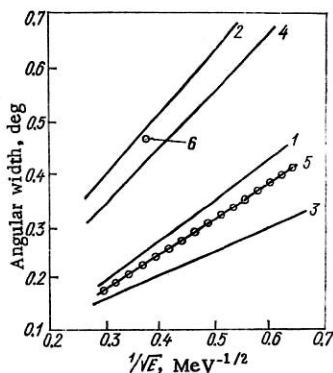


Fig. 3. Calculated angular width of the dip for the $\langle 100 \rangle$ axis of a silicon crystal. 1, 2) Dip width obtained from the equations of ref. 12 for vibrating ($T = 300^\circ\text{K}$) and rigid chains, respectively; 3, 4) width obtained by the method of refs. 10 and 19 for the same conditions; 5, 6) results calculated by the Monte Carlo method for the same conditions.

This potential approach is not as valid for analyzing the blocking effect, since in this case the particles move in the immediate vicinity of the chain axis, so the longitudinal averaging introduces important distortion. In particular, from the form of potential (2) we conclude that the dip width should be infinite. However, this result is found only for a rigid chain; when we take atomic vibration into account, the dip parameters become finite. An explicit analytic expression for the parameter ψ cannot be found in this case, but corresponding integral relations have been found and evaluated by computer. The problem is formulated as follows: The chain is described by a string potential, the emitting atom is a distance $l/2$ from the end of the chain, and its radial displacement is described by a Gaussian distribution. The curves calculated in this manner turn out to also give a qualitatively correct description of the dependences of the dip parameters on various factors. When a model with damped vibration is used, the angle ψ is found to be given by the simple analytic expression

$$\psi = C\psi_1, \quad (4)$$

where $\psi_1 = \sqrt{2b/l}$ is the critical channeling angle, and C is a coefficient whose numerical value lies in the range 1.5-2.

The widths calculated for axial patterns by these two methods were compared with data found by the Monte Carlo method. Figure 3 shows results obtained for the silicon $\langle 110 \rangle$ axis; curves 1, 2, 4, 5 and point 6 are from ref. 20, while curve 3 is from ref. 19. We see that both methods correctly predict the overall behavior of the width as a function of the energy.

As was mentioned above, an extremely important parameter of the dip is the quantity χ ; however, this parameter obviously vanishes for the primary pattern produced by a single infinite chain.

Only the average-potential method has been used to describe the primary chain in the planar case; the potential for a single plane was found in ref. 10. On the basis of the same assumptions used to derive the string potential this potential was found to be

$$Y(y) = 2\pi Z_1 Z_2 N l_p [(y^2 + C^2 a^2)^{1/2} - y], \quad (5)$$

where $N l_p$ is the average number of atoms per unit area of the plane, and y is the coordinate normal for the plane.

The dip shape was calculated numerically in ref. 19 for this potential; as in the previous case, vibration of only the emitting atom was taken into account. Comparison of these results with the Monte Carlo results reveals a qualitative agreement for the shape, but generally no quantitative agreement. No analytic expression has yet been found for the shape of the primary patterns for a discrete plane.

We return now to the second step in the pattern formation. As was mentioned above, the particles forming the primary pattern interact with the crystal as they move toward the crystal surface. The nature of this interaction differs for particles leaving their chains at different angles. If these angles are significantly greater than ψ , the particles move through the crystal as if it were an amorphous medium, and they undergo ordinary multiple scattering. At angles much lower than ψ , particles are captured into the channeling mode. No clear angular boundary can be drawn between these modes; there is a certain intermediate range - "partial channeling" - corresponding to angles approximately equal to ψ . Particles moving at these angles can easily convert from random motion to channeling and vice versa.

An important consideration for the usual method for determining the nuclear lifetime is the relative number of particles which are captured into channeling, since the recoil of compound nuclei from lattice sites affects this quantity. Let us consider in slightly more detail the behavior of particles captured into channeling. From the physics of channeling we know that the trajectories of these particles oscillate. If the particles are emitted from sites at a depth L in a crystal which is comparable to the oscillation wavelength λ , the nature of the angular distribution of these particles after they have escaped from the crystal surface obviously depends on L . Monte Carlo studies (see, e.g., ref. 21) have shown that this dependence vanishes for $L \approx (2-3)\lambda$ in the case of axial patterns and for $L \approx (5-6)\lambda$ in the case of planar patterns. This difference seems natural, since the wavelength λ has a more definite physical meaning in the case of planes. The value of λ has been estimated to be 200-400 Å, so in an actual experiment the depths for which the channeled particles retain definite phase relations are not important. More important is the range of crystal thicknesses characterized by the "statistical equilibrium" introduced in ref. 10. Under these conditions there is a complete phase mixing of trajectories, although the value of E_\perp is conserved for each trajectory. In a real crystal, the situation differs because of dechanneling, but for a depth range of the particles in the crystal the dechanneling is negligible, and the conclusions reached under the assumption of statistical equilibrium can still be used. In particular, using this assumption one can calculate the relative number of channeled particles which leave the crystal precisely along an axial direction, i.e., the contribution to χ from each given category of particles. For a rigid string potential and a vibrating emitter such an estimate yields

$$\chi_1 = N l_p \rho^2, \quad (6)$$

where ρ^2 is the mean square vibration amplitude of the

emitting atom with respect to the chain axis.

For various values of the parameters which appear in Eq. (6), we find χ_1 to be on the order of 1%. This result obviously does not represent the total value of χ . There is a certain probability that particles corresponding to large primary-pattern angles move along the corresponding axes as a result of multiple scattering by surface atoms. For this scattering to occur, the multiple-scattering angle must be larger than ψ_1 ; this condition corresponds to an impact parameter $\leq a$. The contribution to χ from particles in random motion is thus

$$\chi_2 = Nl\pi a^2. \quad (7)$$

It is easy to show that χ_2 and χ_1 are on the same order of magnitude.

The average dip width obviously changes little as a result of these secondary processes; the dip width is governed primarily by multiple scattering of particles corresponding to angles of approximately ψ in the primary pattern. However, in the crystal-thickness range for which the concept of statistical equilibrium is valid, the average multiple-scattering angle turns out to be much smaller than ψ_1 ; hence for crystal thickness corresponding to statistical equilibrium, the ψ values are the same for the resultant and primary patterns, while the χ values turn out to be quite different.

The arguments used for planar patterns are completely analogous, although the quantity χ is of course evaluated differently.

An interesting attempt has been undertaken²¹ to obtain simple expressions for the parameters ψ and χ characterizing the resultant axial and planar patterns through an approximation of the Monte Carlo data. This calculation is carried out under the assumption of statistical equilibrium; energy loss of the particles is neglected.

These results can thus be compared with experiment if relatively thin crystals are used (or if a thick crystal is used, and a narrow region is singled out near the upper limit of the energy spectrum). Under these conditions we find ψ for an axial pattern to be

$$\psi = K [U (mU_1)/E]^{1/2}, \quad (8)$$

where K and m are constants ($K = 0.83$ and $m = 1.2$), u_1 is the amplitude of the thermal vibrations, and $u(x)$ is the string potential. For a planar shadow the value of ψ is

$$\psi = K \{ [Y (mU_1) + Y (l - mU_1) - 2Y (l/2)]/E \}^{1/2}, \quad (9)$$

where $K = 0.76$ and $m = 1.6$. The empirical equations (8) and (9) agree within 3-5% with the Monte Carlo results.

With a further increase in the crystal thickness the particles in random motion undergo pronounced multiple scattering, so some of them move into the small-angle range. The width decreases significantly as a result, while χ increases. Essentially no study has been made of how these conditions affect the possibility of measuring τ .

SOME METHODOLOGICAL QUESTIONS INVOLVED IN DETERMINING THE LIFETIMES OF COMPOUND NUCLEI BY MEANS OF THE BLOCKING EFFECT

The discussion in the preceding section shows that at present we lack a systematic theory for analyzing the effect of the source displacement on the pattern shape. It is therefore not surprising that the efforts to develop this new method have focused on an empirical study of its feasibility. At present more than 20 studies testing the feasibility of this method have been reported,²²⁻⁴⁵ half of which were reported in the last two years.

Turning to an analysis of the various aspects of experimentally determining the lifetime of compound nuclei on the basis of the blocking effect, we note first that since this is a direct method it is applicable at arbitrary excitation energies, both for isolated levels with $\Gamma \ll D$ and in the case $\Gamma \sim D$ or $\Gamma \gg D$, i.e., in the case in which there is a significant level overlap. The studies which have been reported span all the excitation-energy ranges; disregarding the order in which these studies were carried out, we single out as particularly important those experiments in which the lifetimes of isolated resonances have been measured.^{34,40}

The importance of these experiments at this initial stage of the development of this new method lies in the circumstance that these experiments represent the only possible way to test this method by comparison with results found from resonance widths measured directly or calculated on the basis of the yields of the corresponding resonance reactions. We can apparently now conclude that the new method has survived this test: Lifetimes approximately equal to those expected on the basis of the resonance widths have been obtained for two resonance reactions, in one case by two groups of investigators working independently. In the future, measurement of the lifetimes of isolated levels with known widths may be used for an absolute calibration of the widths found by this new method; this possibility is particularly important in the absence of a systematic theory. These measurements may also be used to study the applicability limits of the method at small and large values of τ .

Turning to the question of how the recoil of the compound nucleus from its lattice site affects the pattern shape, we consider the pattern detected over a broad angular range by means of, e.g., a nuclear emulsion. Figure 4 shows a typical pattern, obtained in the scattering of 0.5-MeV protons by a tungsten crystal. We clearly see the dips corresponding to various crystallographic axes and planes. In general, the angular width and the depth of a dip fall off with increasing index of the corresponding crystallographic axis or plane, but the relative depth of a low-index axial dips is generally much larger than that corresponding to a low-index planar dip. Figure 4 also shows that in addition to the axial and planar dips in the pattern there is a characteristic region near an axial dip in which axial and planar dips partially overlap.

It has been established experimentally that all three of these blocking-pattern features are sensitive to the displacement from the lattice sites of the particles which

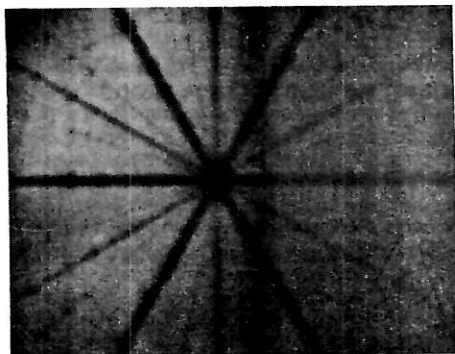


Fig. 4. Blocking pattern obtained in the elastic scattering of 0.5-MeV protons by a tungsten crystal.

eventually form the pattern. For the axial and planar dips proper, the source displacement affects the dip depth most and the angular width least. The effect of the displacement is more pronounced in the axial dips, because they are deeper than the planar dips; this circumstance probably explains why most investigators prefer to work with axial dips. However, it should be noted that in a study of planar dips the experimental difficulties associated with the smallness of the effect may be offset partially by the better statistical accuracy, which results from the use of a large detector aperture along the plane. The effect of the source displacement on the depth of a dip corresponding to a crystallographic axis or plane can be explained qualitatively in a simple manner: Particles emitted from a point at some normal distance from the axis or plane can move along the given axis or plane and can thus cause more pronounced dips.

It is not such a trivial matter to explain the sensitivity to source displacement of the region in which the axial and planar dips partially overlap. Let us consider the reason for the sensitivity of this element of the pattern in the case in which the energy of the particles forming the pattern is not too high, and the dip is formed primarily as a result of scattering by the nucleus nearest the source. In this case the axial pattern corresponds to scattering by a nucleus separated from the source by a

distance on the order of the lattice constant. In the planar case, on the other hand, the first scattering occurs at a point 30-50 times farther away (we are concerned here with the formation of that part of the planar pattern in the immediate vicinity of the axial dip). It follows that for a given normal component of the source displacement the axial dip undergoes a much larger spatial displacement than the planar dip, so the two dips undergo a relative displacement (Fig. 5). In turn, this relative displacement leads to a characteristic asymmetry in the particle distribution in the region of partial overlap. This asymmetry was first observed experimentally in the elastic scattering of low-energy protons (0.2-0.5 MeV) by tungsten nuclei, in which case the recoil of the source from the lattice site can be thought of as corresponding to Coulomb scattering with a large impact parameter.²⁴ An analogous effect was later found in a study of nuclear reactions: the fission of tungsten nuclei by ^{22}Ne ions accelerated to 174 MeV (ref. 37) and the resonance reaction $^{19}\text{F}(p, \alpha)^{16}\text{O}$ with a proton energy of 340 keV (ref. 38); in this case the source displacement was related to the finite lifetime of the compound nucleus.

We turn now to the question of extracting the displacement of the compound nucleus from some element of the blocking pattern. As was mentioned above, the pattern observed experimentally is not the one initially formed, e.g., in the first events in which the particles are scattered by nearest nuclei; instead, this experimental pattern is that produced from the primary pattern by the various factors which operate as the particles move from the interior of the crystal to its surface. Among such factors we must take into account scattering by vibrating atoms of the lattice, the effect of structural defects in the interior of the crystal, the boundary effects which operate as the particle leaves the crystal, and the amorphous structure in the surface layer. Displacement of the compound nucleus from the lattice site is thus one of many factors which are ultimately responsible for the pattern shape. It may be helpful in the effort to single out the "pure" effect of the displacement to compare corresponding elements of two patterns: one obtained under conditions such that all these factors operate and the other obtained under conditions such that all factors except the displacement of the compound nucleus operate. This latter pattern thus becomes a reference point. It is crucial for this comparison to have all the factors other than the displacement of a compound nucleus equally effective in the reference and working patterns.

There are various ways to produce this reference pattern. The most versatile method would apparently be to compare the dip from a crystallographic axis or plane for which the normal component v_{\perp} of the velocity of the compound nucleus is nonvanishing (the working pattern) with the dip from the same axis or plane but oriented with respect to the incident particle beam in such a manner that $v_{\perp} = 0$ (the reference pattern). In the latter case, the normal component of the average recoil displacement of the compound nucleus also vanishes: $s_{\perp} = v_{\perp} \tau = 0$. It would be desirable to have the crystallographic axis (or plane) make the same angle with the surface of the target crystal in both cases, and it would be desirable to obtain both patterns at equal exposure times. If these conditions can be arranged, all the interior and surface effects, e.g.,

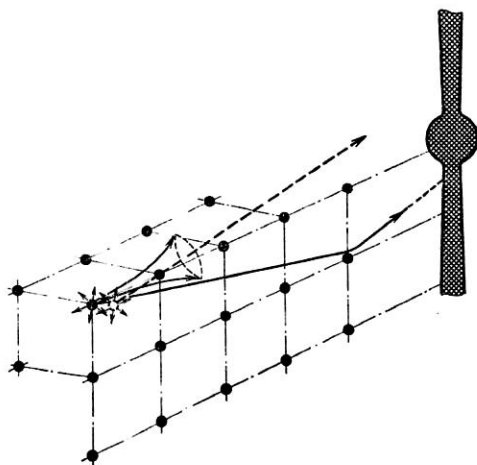


Fig. 5. Diagram used to explain why the region in which axial and planar dips overlap partially is sensitive to the displacement of the compound nucleus from the lattice site.

multiple scattering of particles moving from the interior of the crystal toward the surface, radiation defects, and the state of the crystal surface, would affect the pattern formation in the same manner in both cases.

The condition $s_{\perp} = v_{\perp}\tau = 0$ which is to be met for the reference pattern can also be reached if $\tau \approx 0$; this condition corresponds to observing the dip from a given axis or plane for the products of a reaction which occurs much faster than the reaction being studied. In this experiment the two reactions must produce the same particles at the same energies. For example, a reference pattern for studying inelastic proton scattering could be formed by exploiting the elastic scattering of protons having a suitably lower energy.^{26,31,41} The condition $\tau \approx 0$ could also be reached by measuring τ at a much higher excitation energy of the compound nucleus; this method for producing a reference pattern has been used to study proton-induced fission of uranium nuclei.²⁷ If the characteristic time is measured for a resonance reaction in the immediate vicinity of another, much wider resonance, this latter resonance could be used to produce a reference pattern.³⁴

When the pattern element being studied is the region of partial overlap of the axial and planar dips, the working and reference patterns correspond to two different orientations of the target crystal with respect to the incident beam. In both cases the axis in question is normal to the beam (the beam direction and this axis determine the reaction plane).

In one case the crystallographic plane containing this axis should be normal to the reaction plane (for the working pattern), and in the other case this plane should lie in the reaction plane (for the reference pattern).^{24,37} In the first case the displacement of a compound nucleus from the lattice site (which occurs in the reaction plane) leads to a spatial displacement of the axial pattern with respect to the planar pattern, and there should be an asymmetric distribution of the particle intensity on the different sides of the planar dip. In the second case, on the other hand, there is no relative displacement of the axial and planar dips, so the pattern should be symmetric. All these methods for producing reference patterns have been used experimentally to measure the lifetimes of excited compound nuclei.

After the working and reference patterns have been produced, a parameter having different numerical values in the two patterns must be selected so that the effect of

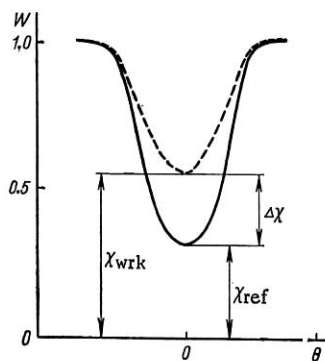


Fig. 6. Reference pattern (solid curve) and working pattern (dashed curve) and the corresponding values of the parameter χ , the intensity at the minimum of the angular distribution ($\Delta\chi$ is the observed effect of the displacement of the compound nucleus).

the displacement of the compound nucleus can be determined. The problem involved here is to find the pattern parameter most sensitive to the displacement, for two reasons: first, to obtain the maximum observable effect for a given displacement, and second, to determine the lower limit on the times measurable by this method.

No detailed study has yet been made of the question of finding the parameter most sensitive to the displacement. Some investigators have used the particle intensity at the dip in the angular distribution, χ (Fig. 6). This choice is apparently traceable to ref. 10, in which a recipe was worked out under certain simplifying assumptions for relating the observed change in χ to the displacement of the source of charged particles from the lattice site. It is customarily assumed that the various factors contribute to χ in an additive manner so that the displacement effect can be found as the difference between the χ values for the working and reference patterns. Generally speaking, this is not an obvious conclusion and it has not been proved. We therefore assign considerable importance to the experimental study of the influence of various factors contributing to χ on the absolute magnitude of the difference between the χ values for the working and shadow patterns, i.e., to the study of the influence of these factors on the magnitude of the effect of the displacement.

It has been found that the difference $\Delta\chi$ is extremely stable with respect to large changes in such factors as multiple scattering and lattice defects. This conclusion follows, first, from the essentially constant value of $\Delta\chi$ for different depths of the working layer of the target. These depths were chosen by recording various regions of the reaction-product (fission-fragment) energy spectrum by placing retarding foils in front of a detector. Second, the use of target crystals differing in degree of perfection and having χ values from 0.12 to 0.38 revealed no appreciable change in $\Delta\chi$. Although these results are encouraging, this study should be pursued.

An alternative to the experimental study of the sensitivity of the displacement to various factors is to seek parameters displaying the least sensitivity to these factors, through a theoretical analysis of particle motion in a crystal on the basis of appropriate models. Interesting results have been obtained very recently: It has been found that in the case of the planar pattern one can construct a combination of parameters of the working and reference patterns which is essentially independent of the depth of the working target layer, i.e., this combination of parameters is essentially independent of multiple scattering which occurs as the particles move toward the crystal surface.⁴² This unusual invariant is the quantity $(1 - \chi_{\text{wrk}})/(1 - \chi_{\text{expt}})$.

A certain integral characteristic of the pattern has been adopted in certain studies as a quantitative measure of the displacement. Use of this characteristic involves calculating the relative number of particles in a certain angular range near a crystallographic axis³¹ or plane²⁶ "ejected" as a result of Coulomb interactions with nuclei in this axis or plane. The ratio of the values of this characteristic for the working and reference shadows serves as a quantitative measure of the displacement effect (Fig. 7).

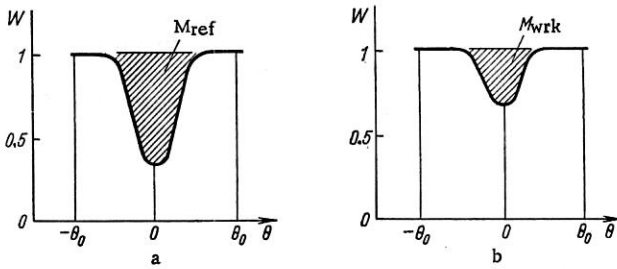


Fig. 7. Reference (a) and working (b) patterns and the corresponding values of the integral parameter M , proportional to the number of particles "ejected" as a result of Coulomb collisions with atoms of the crystallographic axis or plane from a certain angular interval.

An extremely important aspect of this method, yet one which has received very little study, is the conversion from the observed effect to the average displacement of the compound nucleus. Lacking a systematic theory for the passage of charged particles through a crystal which takes sufficient account of the various factors involved, essentially all investigators developing analytic models for calculating this average displacement on the basis of the observed effect have based their arguments on Lindhard's study,¹⁰ which contains extremely important simplifications. For example, a cutoff radius r_c for the potential of the atomic chain was introduced in ref. 27. It was assumed that particles emitted by the compound nucleus beyond r_c can move freely along the corresponding crystallographic axis and make a definite contribution to χ , given by χ_1 . If, on the other hand, the source displacement, s , does not exceed r_c , the effect of this displacement on the observed particles intensity at the center of the dip is given, by analogy with the effect of thermal vibrations of the chain atoms, by $\chi_2 = \pi Nd \langle s^2 \rangle$, where N is the atomic density in the crystal, and d is the spacing of atoms in the chain. The overall particle intensity at the center of the dip due to displacement of a compound nucleus undergoing exponential decay is

$$\Delta\chi = \chi_1 + \chi_2 = \exp[-r_c/(v_\perp\tau)] + C\pi Nd \int_0^{r_c} s^2 \exp[-s/(v_\perp\tau)] ds / (v_\perp\tau), \quad (10)$$

where the factor $C \approx 2.5$ is introduced to correct the truncated-potential model used to approximate the potential of the atomic change.⁴⁶ The cutoff radius is chosen equal to roughly three times the screening parameter of the Thomas-Fermi atomic potential. This procedure obviously involves some arbitrariness - a basic shortcoming of this approach.

Another method for relating the displacement of the compound nucleus to the intensity at the minimum of the angular distribution near a crystallographic axis was proposed by Melikov.³³ In this method the problem of finding the probability that a particle emitted from a displaced nucleus will move along a given crystallographic axis is replaced by a calculation of the probability that a particle moving between atomic rows in the crystal parallel to the given crystallographic direction will strike the displaced nucleus. This analysis uses a continuous potential for the atomic chain, and it assumes that a statistical equilibrium is established in the transverse plane of phase

space immediately after the particle reaches the crystal. The desired probability is then found from the equation

$$W(s) = \int_{E_\perp > U(s)} P(E_\perp, s) f(E_\perp) dE_\perp = \frac{1}{\pi r_0^2} \ln \left(\frac{1}{1 - s^2/r_0^2} \right), \quad (11)$$

where s is the normal component of the nuclear displacement, E_\perp is the transverse energy of the particle, $U(s)$ is the potential of the nearest atomic chain, $P(E_\perp, s)$ is the probability that a particle with a transverse energy E_\perp lies at a distance s from the chain, $f(E_\perp)$ is the particle distribution function in to the transverse energy, and $\pi r_0^2 = (Nd)^{-1}$ is the area of the transverse plane per chain. For a particle entering a crystal at a sufficiently large angle with respect to the atomic chain, the motion in the crystal is essentially the same as in a material lacking atomic order, and the analogous probability is $W_0(s) = 1/(\pi r_0^2)$. When an exponential law is adopted for the decay of the compound nucleus, the following expression is found for the relative particle intensity at the center of the axial dip due to the nuclear displacement:

$$\begin{aligned} \Delta\chi(v_\perp\tau) &= C \int_0^\infty \frac{W(s)}{W_0(s)} \exp[-s/(v_\perp\tau)] \frac{ds}{v_\perp\tau} \\ &= \frac{C}{v_\perp\tau} \int_0^{r_0} \exp[-s/(v_\perp\tau)] \ln \left(\frac{1}{1 - s^2/r_0^2} \right) ds \\ &\quad + \frac{C}{v_\perp\tau} \int_{r_0}^{3r_0} \exp[-s/(v_\perp\tau)] \ln \left[\frac{1}{1 - (2r_0 - s)^2/r_0^2} \right] ds + \dots \quad (12) \end{aligned}$$

It can be shown that if the average nuclear displacement is small, namely, if $v_\perp\tau \lesssim 0.4r_0$, we have

$$\Delta\chi(v_\perp\tau) \approx 2C\pi Nd (v_\perp\tau)^2. \quad (13)$$

The most important simplifications incorporated in this solution are the use of the string-potential approximation for the chain and the requirement that a statistical equilibrium be rapidly established in the transverse plane of phase space. This approach and that based on the introduction of a cutoff radius for the potential yield approximately equal results if the average nuclear displacement is on the order of the atomic-screening parameter.

The observed effect of the displacement of the compound nucleus was related analytically to the magnitude of the displacement in the case of a planar pattern by Komaki and Fujimoto.⁴³ This relation is also based on the string potential and a statistical equilibrium with respect to the transverse particle energy. In this case the measurable parameter is the relative number of particles ejected from a certain angular range near the direction of the plane as the result of Coulomb collisions with the plane (Fig. 7). Using conservation of the number of particles we can replace these particles by those which turn out to lie outside this angular range. If the boundaries of this range, θ_0 , are much larger than those corresponding to the angular size of the dip, we find an analytic expression for the angular distribution of particles for $\theta > \theta_0$; we can use this expression to relate the distribution function $g(x, v_\perp\tau, \rho)$ of the particle source (i.e., the position of the decaying compound nucleus) to the relative number of ejected particles $M[\theta_0, g(x, v_\perp\tau, \rho), E]$:

$$M(\theta_0, g(x, v_{\perp}\tau, \rho), E) \approx \frac{1}{E\theta_0^2} \{\alpha[g(x, v_{\perp}\tau, \rho)] - \beta\}, \quad (14)$$

where

$$\alpha[g(x, v_{\perp}\tau, \rho)] := \int_{-\infty}^{\infty} g(x, v_{\perp}\tau, \rho) U(x) dx; \quad \beta = \frac{1}{d} \int_0^d U(x) dx.$$

Here E is the energy of the particles emitted by the nucleus, $U(x)$ is the average potential of the atomic plane, and d is the separation between planes. The distribution function for the position of the particle source takes into account the displacement due to the finite lifetime of the compound nucleus as well as the displacement due to thermal vibrations of atoms:

$$g(x, v_{\perp}\tau, \rho) = \frac{1}{\sqrt{2\pi}\rho v_{\perp}\tau} \int_0^{\infty} \exp[-(x-x')^2/(2\rho^2)] \exp[-x'/(v_{\perp}\tau)] dx'. \quad (15)$$

where $v_{\perp}\tau$ is the normal component of the average nuclear displacement, and ρ is the transverse component of the rms amplitude of the thermal vibrations. Experimentally obtaining working and reference planar patterns, we can find the ratio of the corresponding M values:

$$\frac{M(\theta_0, g(x, v_{\perp}\tau, \rho), E)}{M(\theta_0, g(x, 0, \rho), E)} = \frac{\alpha[g(x, v_{\perp}\tau, \rho)] - \beta}{\alpha[g(x, 0, \rho)] - \beta}. \quad (16)$$

Since this ratio is a function of displacement $v_{\perp}\tau$, it relates the observed effect of the displacement to the magnitude of the displacement.

In another approach to the problem of calculating the lifetime on the basis of the observed effect, the particle motion in the crystal is simulated in a Monte Carlo calculation; in principle, this approach allows us to trace the dependences of the pattern shape and parameters on the displacement of the compound nucleus from the lattice site.^{44,45} With the problem formulated sufficiently accurately, and with a good statistical accuracy, this method seems very promising, not only for calculations related to specific experiments, but also for studying the question of which pattern parameters are most sensitive to the nuclear displacement. The primary difficulties involved here result from the sharp increase in the computer time required for the numerical calculations as the actual experimental conditions are approached. At present calculations have been carried out only for thin crystals (thinner than those used in experiments by a factor of about 100), i.e., the role of multiple scattering in forming the shadow has been neglected.³¹

In completing this discussion of method for calculating the average lifetime we note that an exponential decay law is satisfactory for the compound nucleus only if a single isolated resonance is excited.⁴⁷ Since lifetime measurements based on the blocking effect are applicable in any part of the excitation spectrum for the compound nucleus, the most typical situation would involve the excitation of many closely spaced levels, and the decay probability would have a nonexponential distribution.⁴⁸

It follows that the effect of the finite lifetime of the compound nucleus is manifested in the angular distributions of the reaction products as a second-order effect; first-order effect would be the appearance of the inten-

sity along the crystallographic axes and planes (i.e., the dips themselves). An experimental method for detecting small changes in dip shape due to displacement of the compound nucleus from the lattice site must of course satisfy certain specific requirements. The most important of these are a sufficient spatial (on angular) detector resolution, especially if the element of the pattern being studied is the region in which the axial and planar dips overlap; insensitivity of the detector to particles making up the background against which the particles from the given reaction must be distinguished; highly accurate positioning of the target in the case in which the angular distribution near the given axis or plane is found by successive measurements; and monitoring of the target state, especially if the working and reference patterns are not measured simultaneously. Obviously, the angular distributions of reaction products obtained must have a sufficiently low statistical error.

Two types of detectors have been used to obtain patterns for measuring nuclear lifetimes: dielectric track detectors and position-sensitive semiconducting detectors. Dielectric track detectors are absolutely insensitive to background particles, while they have an essentially 100% efficiency for detecting the reaction products. Their use is simple and convenient. These detectors can simultaneously obtain blocking patterns over a broad angular range, thereby eliminating positioning errors. They suffer from the important disadvantage that they cannot be used for an energy analysis of the reaction products, so they cannot determine the depth of the working layer of the target when a thick crystal is used. In (p, α) reactions the α particles are detected by cellulose nitrate detectors, while the fission fragments are detected by silicate and quartz glass and polymer plates. Position-sensitive semiconducting detectors can simultaneously obtain information about both the spatial and energy distributions of the reaction products. Two-dimensional "checkerboard" detectors have been used to measure the angular distributions of particles near crystallographic axes, while planar patterns have been measured with detectors sensitive to a single coordinate.

Use of a position-sensitive detector requires more careful orientation of the crystal than does the use of a large-area dielectric track detector. Preliminary orientation of the crystal is usually carried out in these experiments by observing the blocking patterns from elastically scattered particles either on a fluorescent screen or by means of a photographic emulsion. The target crystal is mounted on a goniometer table, which sometimes must have translational as well as rotational degrees of freedom. Translational degrees of freedom are necessary because crystal unstable with respect to radiation must be used to study certain nuclear reactions. If the dose per unit area of the crystal surface is not to exceed the permissible limit, the crystal must be displaced with respect to the particle beam; the spatial orientation of the crystallographic axes and planes must not change as a result of this displacement.

We turn now to the geometry of these experiments. In a "good" geometry the linear dimensions of the spot formed on the target by the incident beam are much smaller than the linear dimensions of the elements of the

pattern being studied; in other words, the angular resolution of the apparatus must be much finer than the angular width of the dip. Otherwise, the dips would suffer instrumental broadening and would be less pronounced.

It can be shown that the change in the depth of an axial dip due to geometric factors is³⁶

$$\delta\chi = (1 - \chi)(a^2/b^2)/6, \quad (17)$$

where a is the diameter of the projection of the irradiated spot on the target onto the plane parallel to the detector plane, and b is the diameter of the axial dip on the detector surface. The standard statistical error in the quantity $\Delta\chi$, the difference between the intensities at the dips of the working and reference patterns, can be written as

$$\delta(\Delta\chi) = (\delta A_1/A_1 + \delta B_1/B_1)(A_1/B_1) + (\delta A_2/A_2 + \delta B_2/B_2)(A_2/B_2), \quad (18)$$

where A_1 and A_2 are the particle intensities at the centers of the dips, and B_1 and B_2 are the intensities away from the dips, so that we have $A_1/B_1 = \chi_1$ and $A_2/B_2 = \chi_2$. Estimates show that with an angular resolution equal to $1/10$ the angular width of the dip we have $\delta\chi \leq 0.01\chi$, and this error does not make a contribution to $\Delta\chi$ important in comparison with the statistical contribution. In particular, it follows that the beam of incident particles must be quite narrow, so the problem of radiation defects is compounded. It is also quite clear that repeated displacement of the target crystal during an exposure can lead to inadvertent small changes in the positions of the crystallographic axes and planes; in turn, these changes could distort pattern features. To eliminate such undesirable effects, certain investigators have continuously monitored the spatial position and depth of some pattern other than that being studied during the exposure, using position-sensitive semiconducting detectors. The effect of radiation defects can also be reduced by annealing, i.e., by heating the target crystal during the recording of the pattern. An undesirable consequence is that the pattern contracts and fades because of the increased amplitude of thermal vibrations caused by the heating. Nevertheless, this procedure makes repeated translations of the crystal unnecessary. In general, the problem of radiation defects and their effect on the pattern shape seems to be one of the most serious experimental difficulties involved in measuring nuclear lifetimes with crystal targets.

REVIEW OF BLOCKING-EFFECT MEASUREMENTS OF NUCLEAR REACTION TIMES

All the experiments which have been carried out to determine the lifetimes of excited nuclear states can be classified into three groups on the basis of the nature of the reaction studied. The first group includes measurements of the lifetimes of isolated levels in resonance reactions: $^{31}\text{P}(p, \alpha)^{28}\text{Si}$ at $E_p = 642$ keV (ref. 40) and $^{27}\text{Al}(p, \alpha)^{24}\text{Mg}$ at $E_p = 633$ keV (refs. 34, 40). The second group consists of studies of the inelastic scattering of protons having energies of 4–6 MeV by the germanium isotopes ^{70}Ge , ^{72}Ge , and ^{74}Ge (refs. 26, 31, 41). The third and largest group is made up of studies of the fission of heavy nuclei (refs. 23, 25, 27–30, 32, 33, 35–37, 39, and

40). We will discuss each of these groups of reactions in turn.

1. The (p, α) reactions have been studied with protons accelerated by electrostatic accelerators. The targets have been thick (~ 1 mm) GaP and Al single crystals. In the case of a resonance reaction the crystal thickness is not crucial, since it is always possible to induce the reaction at the desired depth in the crystal by making the appropriate change in the energy of the incident particles. As a rule, the proton energy has been about 10 keV above the resonance, so that the reaction has occurred at a depth of about 1500 Å in the crystal. This imbedding of the resonance was necessary because at a crystal surface there is an amorphous oxide film or a thin layer of amorphous matrix material; this layer remains even after the crystal surface is carefully prepared before an experiment. The crystal was oriented in such a manner that one of its axes^{34,40} or planes³⁴ made a small ($< 10^\circ$) angle with the direction of the incident beam, while another axis or plane of the same type made a large angle with the beam, i.e., in this setup reference and working patterns could be obtained simultaneously. Figure 8 shows a typical experimental setup. The patterns were obtained with cellulose nitrate dielectric detectors. As a rule, an exposure lasted 30–40 h at an average current of 0.1–0.5 μA at the target. During this exposure time the crystal was moved several hundred times to avoid radiation defects. Position-sensitive semiconducting detectors were used during these several hundred parallel displacements to monitor the crystal orientation (to hold it constant) and to check for a possible change in the dip depth due to radiation defects (Fig. 8). Since the angles made with the crystal surface by the two axes being studied were not held equal,⁴⁰ it was important to verify that the conditions governing the motion of the particles along these two axes were identical when the displacement of the compound nucleus from the lattice site played no role. For this purpose patterns were obtained at the resonance energy of 1.51 MeV in the case of the $^{31}\text{P}(p, \alpha)^{28}\text{Si}$ reaction; the width of this resonance is about 7 keV, so a lifetime of about 10^{-19} sec should lie beyond the sensitivity of the method (or at least this lifetime should not change the shadow depth). The results shown in Fig. 9a show that the intensities in the two directions are in fact identical when the reaction products are emitted almost exactly at the lattice sites. On the other hand, Fig. 9b clearly shows the effect of nuclear displacement for the resonance at 642 keV. The low radiation stability of the crystal and the low α yield in the reaction (about 10^5 protons are required per α , even for back

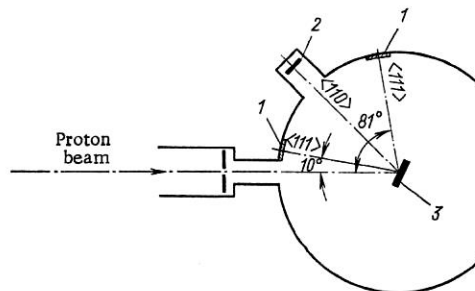


Fig. 8. Experimental setup used to study⁴⁰ the resonance reaction $^{31}\text{P}(p, \alpha)^{28}\text{Si}$. 1) Track detector; 2) position-sensitive semiconducting detector; 3) GaP crystal.

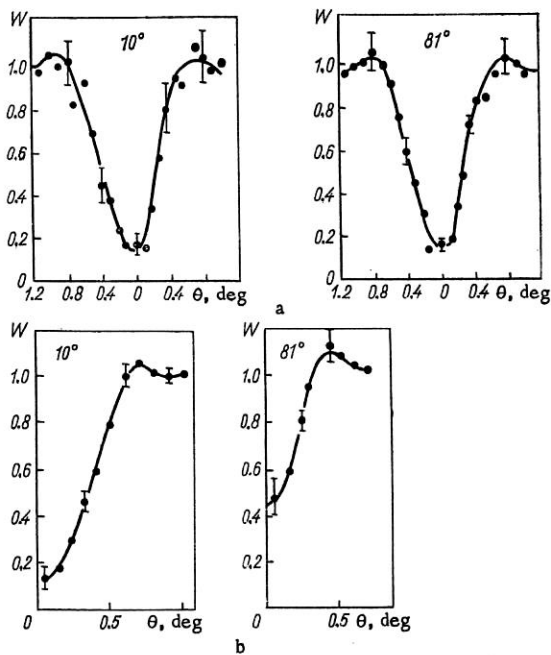


Fig. 9. Blocking patterns obtained⁴⁰ in a study of the resonance reaction $^{31}\text{P}(p, \alpha)^{28}\text{Si}$ at $E_{\text{res}} = 1.51$ MeV (a) and $E_{\text{res}} = 642$ keV (b).

scattering) are responsible for the large statistical error in these results. To obtain clear radial dip profiles in the face of this large error, an integration was carried out over the azimuthal angle near the center of the dip; the results are the angular distribution shown in Fig. 9b. The lifetime of the ^{32}S compound nucleus was calculated on the basis of Eq. (13).

Various methods have been used to measure the effect of the finite lifetime of the compound nucleus in the reaction $^{27}\text{Al}(p, \alpha)^{24}\text{Mg}$ at a resonance proton energy of 633 keV. A comparison has been made³⁴ of the integral characteristics for the two planar patterns (see the preceding section) formed by (111) planes with vanishing and nonvanishing normal components of the compound-nucleus velocity; the lifetime was calculated from Eq. (16). The dip from a $\langle 110 \rangle$ axis was also observed in that study; this dip was used as a reference dip in a comparison with the dip from the same axis corresponding to a different resonance ($E_{\text{res}} = 1183$ keV). This resonance has a width of $\Gamma \approx 650$ eV and a lifetime of $\tau \approx 10^{-18}$ sec. The τ was calculated by a method involving a cutoff radius for the atomic potential. Two axial dips from $\langle 111 \rangle$ axes making angles of 15° and 75° with the direction of the incident

proton beam were obtained⁴⁰ for the same reaction at a resonance energy of 633 keV. The lifetime was calculated from Eq. (13). Table 1 shows the results found from measurements of the lifetime of isolated compound-nucleus states. The accuracy of these lifetimes is limited not so much by the statistical errors involved (generally 10-20%) as by the approximations used to convert from the experimentally measured effect of the displacement to the mean lifetime. Since the results shown in Table 1 were obtained in studies of different pattern elements, and since different methods were used to calculate τ , we believe that the agreement of these results [for the reaction $^{27}\text{Al}(p, \alpha)^{24}\text{Mg}$] and the agreement between the values found from the resonance widths are completely satisfactory.

2. Inelastic proton scattering by germanium isotopes has been studied by three groups of investigators^{26,31,41} over the energy range 5-6 MeV. The compound nuclei ^{71}As and ^{73}As formed in the respective reactions $^{70}\text{Ge}(p, p')$ and $^{72}\text{Ge}(p, p')$ have excitation energies of 9.4-10.4 and 10.3-11.3 MeV. In this excitation-energy range we have the relation $\bar{\Gamma} < \bar{D}$, and the average level spacing is on the order of hundredths of an electron volt. The germanium crystals were "thin," i.e., their thickness was a negligible fraction of the proton range. However, the energy spread caused in the scattered protons by the target thickness (about 200 keV at a crystal thickness of about^{26,31} 10μ and about 30 keV at a thickness of about⁴¹ 1.5μ) resulted in the simultaneous excitation of a large number of levels of the compound nucleus.

The germanium crystal was oriented with its $\langle 110 \rangle$ axis^{31,41} or (111) plane²⁶ making an angle of about 90° with the direction of the incident proton beam. The angular distribution or patterns were measured near this axis and this plane with position-sensitive semiconducting detectors. The groups of inelastically scattered protons corresponding to the 1.04-MeV (2^+) state in ^{70}Ge and the 0.69-MeV (0^+) and 0.83-MeV (2^+) states in ^{72}Ge were singled out. The effect of the finite duration of the inelastic-scattering process was extracted by comparison with the pattern formed by elastically scattered protons whose energy was reduced to equal that of the corresponding group of inelastically scattered photons.

Figure 10 shows two of these patterns.⁴¹ Since germanium crystals have a high radiation stability, they did not have to be moved during the exposure. However, even with these crystals it was necessary to take measures to prevent changes in the pattern shape caused by factors other than the effect being studied. The crystals deformed

TABLE 1. Results of Experiments Carried Out to Determine the Lifetimes of Resonances

Reaction	Resonance proton energy, keV	Compound nucleus	Excitation energy, MeV	Pattern element studied	Measured mean lifetime, 10^{-16} sec	Lifetime calculated from resonance width, 10^{-16} sec	Reference
$^{31}\text{P}(p, \alpha)^{28}\text{Si}$	642	^{32}S	9.486	Axial pattern	0.8	~ 0.8	[40]
$^{27}\text{Al}(p, \alpha)^{24}\text{Mg}$	633	^{28}Si	12.21	Planar pattern	1.4	~ 0.4	[34]
				Axial pattern	2		[34]
				Axial pattern	0.9		[40]

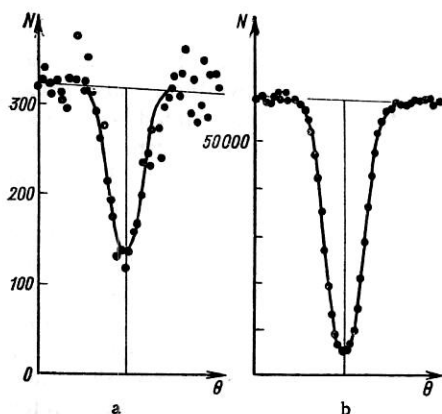


Fig. 10. Blocking patterns from the $\langle 110 \rangle$ axes of a germanium crystal in the reaction $^{70}\text{Ge}(p, p')^{70}\text{Ge}^*$ (0.83 MeV) with $E_{\text{res}} = 5.11$ MeV (a) and in elastic scattering of protons (b) (ref. 41).

slightly as a result of local heating by the proton beam; this deformation tended to change the spatial position of the crystallographic axis being used and thus to affect the pattern shape. To prevent these changes it was necessary to limit the proton current to about³¹ 0.005 μA . When crystal was heated to about 450°C, on the other hand, the effect of local heating by the beam was much less pronounced, so the current could be raised to about⁴¹ 0.1 μA .

Various methods were used to calculate the mean lifetimes of the compound nuclei in these three studies. In the case of the planar patterns²⁸ a relation was used between the mean nuclear displacement and integral pattern characteristic (16). For axial patterns Eq. (10) was used with a cutoff radius of $r_c = 0.4 \text{ \AA}$ in one case;⁴¹ in the other case³¹ the relative number of particles ejected as a result of Coulomb interactions of elastically and inelastically scattered protons with the crystallographic axis was compared with the analogous numbers obtained through a numerical simulation for various mean displacements of the compound nucleus. Some of these results are shown in Table 2.

3. A large number of studies have been reported (refs. 23, 25, 27, 28-30, 32, 33, 35-37, 39, and 40) in

TABLE 2. Measured Lifetimes of Compound Nuclei Formed in the Inelastic Scattering of Protons by Germanium

Reaction	Energy of incident protons, MeV	Compound nucleus	Excitation energy, MeV	Pattern element used	Measured mean lifetime, 10^{-17} sec	Reference
$^{70}\text{Ge}(p, p')^{70}\text{Ge}^*$ (1.04 MeV 2^+)	5.4	^{71}As	9.64—9.84	Planar pattern	(3.2 ± 1.4)	[26]
	_____			Axial pattern	(2.4 ± 0.4)	[31]
	5.11		9.53—9.56	Axial pattern	(5.4 ± 0.4)	[41]

$^{72}\text{Ge}(p, p')^{72}\text{Ge}^*$ (0.83 MeV 2^+)	5.4	^{73}As	10.54—10.74	Planar pattern	(2.5 ± 1.0)	[26]
	_____			Axial pattern	(3.9 ± 0.7)	[31]
	5.11		10.42—10.45	Axial pattern	(8.1 ± 0.5)	[41]

which the blocking effect has been used to measure the lifetimes of compound nuclei in fission reactions. There are good reasons for the interest in the fission of heavy nuclei, which was among the earliest processes studied by this new method. First, it is customarily assumed that fission occurs only through the formation of a compound nucleus, so that the contribution of direct-interaction mechanisms can be neglected. Second, fission fragments, which have large charges and masses, can be easily distinguished from all other reaction products through the use of zero-background yet simple threshold detectors such as dielectric track detectors. Finally, the large charge of the fragments at the comparatively low energy of about 1 MeV/nucleon provides a large angular width for the dips, which facilitates shape studies.

Measurements of the lifetimes of fissioning nuclei can be classified into two categories: The first includes experimental studies of the fission of ^{238}U nuclei by neutrons,^{28,33,39,40} protons,^{23,27} and alphas,²⁵ with excitation energies of the compound nuclei in the range 6.5-20 MeV. The second category includes experiments^{29,30,32,35-37} using heavy-ion beams of ^{11}B , ^{12}C , ^{16}O , ^{22}Ne , and ^{31}P , in which the excitation energies of the compound nuclei, having $79 \leq Z \leq 89$, exceed 60 MeV.

We turn first to fission at relatively low excitation energies. The first such experiments involved fission of ^{238}U nuclei in a UO_2 crystal of natural isotopic composition caused by 12-MeV protons^{23,27} or 15-MeV α particles.²⁵ The experimental layouts were similar to that shown in Fig. 8. The fission fragments were detected by dielectric track detectors. Analysis of these detectors revealed quite deep minima in the track-density distribution at the detector surface where the detector plane was intersected by the crystallographic $\langle 110 \rangle$ axis. The very existence of dips, which shows that the displacement of the compound nucleus does not exceed the atomic-screening parameter in order of magnitude, yielded an upper limit of $\tau < 10^{-17}$ sec on the lifetimes of the compound nuclei for an excitation energy of about 20 MeV.

Let us summarize the most important results of these early experiments. First, observation of extremely deep dips in the angular distributions of these fragments showed that use of the blocking-effect method was promising for studying the lifetimes of fissioning compound nuclei. Before these experiments it was feared that the high scattering cross section for fragments moving in a medium and possible radiation damage to the crystal by the fragments would cause an extremely poor dip depth. Second, the first use was reported²⁵ of certain methodological approaches which later were widely adopted in quantitative studies of dip shape. One of these approaches involved visual observation of the patterns produced by fission fragments at the surface of glass detectors with a sufficiently high density of fragment tracks (Fig. 11). This approach made it easy to find the pattern elements of interest.

The $^{238}\text{U}(p, f)$ reaction was later studied²⁷ in more detail through the use of protons at 9-12 MeV. It was found that the dip corresponding to the $\langle 111 \rangle$ axis, which made an angle of 40° with the proton-beam direction, was less pronounced at a proton energy of 10 MeV than at an energy of 9 or 12 MeV (Fig. 12). These results have been

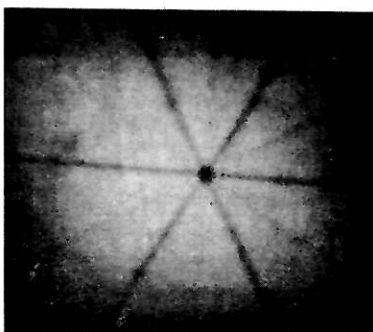


Fig. 11. Blocking pattern observed in the fission of uranium nuclei of a UO_2 crystal by 25-MeV α particles.²⁵

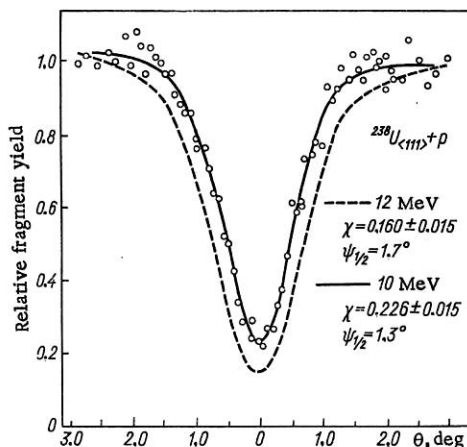


Fig. 12. Comparison of blocking patterns near the $\langle 111 \rangle$ axis of a UO_2 crystal, at an angle of 40° with respect to the proton beam (proton energies of 12 and 10 MeV) corresponding to the reaction $^{238}\text{U}(p, f)$ (ref. 27).

interpreted²⁷ in the following manner: The compound nucleus ^{239}Np formed by a 10-MeV proton and a ^{238}U target nucleus has an excitation energy above 15 MeV, so its lifetime is too short to affect the dip depth. In this case, however, emission fission also becomes possible after

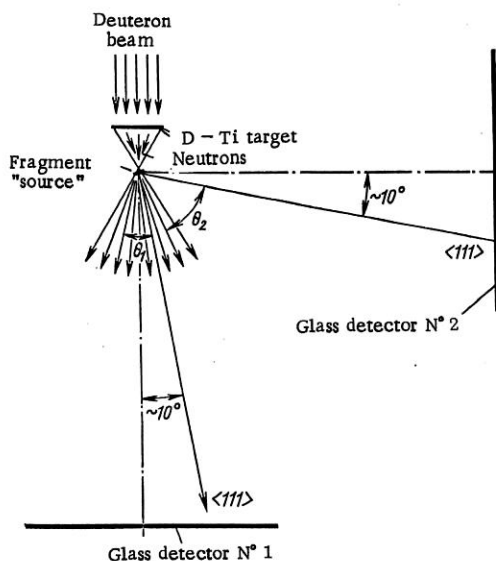


Fig. 13. Experimental setup for measuring the lifetime of the compound nucleus formed in the reaction $^{238}\text{U}(n, f)$ at a neutron energy of 1.7 MeV (ref. 33).

the ^{239}Np nucleus emits a neutron; the ^{238}Np product has an excitation energy not far above the fission barrier, and the quite long lifetime can be measured. Accordingly, the dip depth observed at a proton energy of 10 MeV results from a significant contribution from fission after neutron emission.

For a proton energy of 9 MeV the compound nucleus ^{239}Np also has a very short lifetime, not measurable by the blocking effect; the ^{238}Np nucleus formed after neutron emission has an excitation energy below the fission barrier, and therefore the $^{238}\text{U}(p, n\bar{f})$ reaction is suppressed. At a proton energy of 12 MeV the mean excitation energy of the compound nucleus after neutron emission is considerably above the fission barrier, and the extremely short duration of the emission fission $^{238}\text{U}(p, n\bar{f})$ cannot be measured by this method. Accordingly, for proton energies of 9 and 12 MeV, displacement of the compound nucleus does not affect the pattern shape (the "reference pattern"), while at 10 MeV the effect of the displacement is observable. The results of this experiment and the known values of the ratio Γ_n/Γ_f for this reaction led to a mean lifetime of $(1.4 \pm 0.6) \cdot 10^{-16}$ sec for ^{238}Np for an excitation energy of about 7 MeV. The lifetime was calculated by a method using an atomic potential cutoff radius at $r_c = 0.4 \text{ \AA}$.

The results of refs. 23, 25, and 27 imply that in fission of uranium by light particles conditions are suitable for lifetime measurements by means of the blocking effect only when the compound nuclei involved have low excitation energies, near the fission barrier. The most natural method for producing such excitation energies for the fissioning nucleus is to use monoenergetic neutrons having energies on the order of a few MeV. Two groups of investigators have carried out corresponding experiments in the neutron-energy range 1.7–4.2 MeV, corresponding to excitation energies of the compound nucleus ^{239}U in the range 6.5–9.0 MeV (refs. 28, 33, 39, 40). The neutrons are produced in reactions induced by accelerated charged particles. The reaction $^3\text{H}(p, n)^3\text{He}$ has been used to produce neutrons having energies of 1.7 (ref. 33), 1.8 (ref. 40), and 2.5 MeV (ref. 40). The $^2\text{H}(d, n)^3\text{He}$ reaction has yielded neutrons having 3.3 (ref. 28) and 4.2 MeV (ref. 39). Figure 13 shows the typical experimental layout. The layout for neutron-fission experiments has several features, related to collimation of the neutron beam which distinguish it from experiments involving fission by charged particles. When appropriate diaphragms are used in the charged-particle experiments it is easy to specify both a strictly defined direction for the incident beam (and thus the momentum direction of the compound nucleus) and the size of the spot on the target crystal which is the source of reaction products, in particular, the source of fragments. When fission is induced by neutrons, on the other hand, the neutrons irradiate the entire target crystal, so that the entire crystal emits fission fragments. Since a "good" geometry is required for observing the blocking patterns, i.e., since the source dimensions must be much smaller than the linear dimensions of the blocking pattern at the detector surface, the area of the crystal surface which emits fragments must be restricted. The usual measure is to use a foil mask with an aperture; the foil thickness is chosen to be larger than the fragment range, and the size of the aperture (the fragment source) must satisfy the requirements for good geometry. The crystal

is usually placed very close to the deuterium or tritium target which serves as the neutron source, to maximize the intensity of the neutrons inducing the fission. The geometric conditions are unsatisfactory in another sense: The compound nuclei whose fission fragments can escape from the aperture in the mask do not have a strictly defined momentum direction; instead the momenta are spread over a cone whose vertex angle is governed by the diameter of the aperture and the distance between the fragment source and the neutron source (Fig. 13). As a result, there is a certain spread of angles between the given crystallographic direction and the direction of the compound-nucleus momenta which must be taken into account when calculating the lifetime τ from the observed change in shadow shape. For example, if the measured parameter is the particle intensity at the center of the dip, the quantity $\chi(v_{\perp}\tau)$ must be replaced by

$$\tilde{\chi}(v_{\perp}\tau) = \int \chi(v_{\perp}\tau) g(\theta) d\Omega / \int g(\theta) d\Omega, \tag{19}$$

where θ is the angle between the momentum direction of one of the compound nuclei and the crystallographic direction being used, and $g(\theta)$ is the direction distribution of the compound nucleus momenta. Then the experimentally measured effect of the finite lifetime, $\Delta\chi$, must be equated to the difference between two expressions like (19):

$$\Delta\chi = [\tilde{\chi}(v_{\perp}\tau)]_{\vartheta_1} - [\tilde{\chi}(v_{\perp}\tau)]_{\vartheta_2}, \tag{20}$$

where ϑ_1 is the angle between the axis of the cone formed by the compound-nucleus momenta and the crystallographic axis forming the working pattern, and ϑ_2 is the same angle for the reference pattern.³³ A study was made of patterns from the $\langle 111 \rangle$ axes of a UO_2 crystal, one making an angle of $\vartheta_1 = 80^\circ$ with the cone axis and the other making an angle $\vartheta_2 = 10^\circ$. Figure 14 shows the angular distributions of fragments near these axes, integrated over the azimuthal angle, for a neutron energy of 1.7 MeV; here the UO_2 crystal was irradiated by a neutron flux of about $1.5 \cdot 10^8$ neutrons/(sec·sr) for 120 h. There is a clear difference between dip depths, which can be attributed only to the effect of the displacement of the fissioning nuclei from the lattice sites. The lifetime calculated from Eqs. (12) and (13) for the compound nucleus ^{239}U excited to 6.5 MeV turned out to be³³ $\tau = (3.5 \pm 1.0) \cdot 10^{-16}$ sec. Similar re-

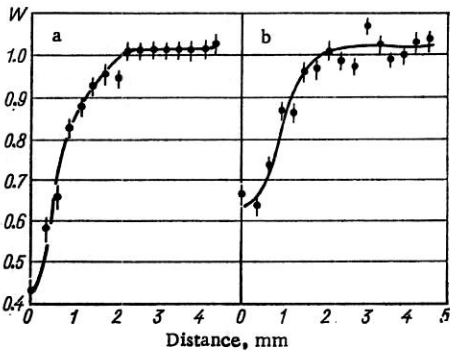


Fig. 14. Portions of the angular distributions, integrated over the azimuthal angle, of the fission fragments produced by the irradiation of a UO_2 crystal by 1.7-MeV neutrons. These parts of the distributions lie near the $\langle 111 \rangle$ axes, oriented at an angle of 10° with respect to the beam direction (a) and at an angle of 80° (b) (ref. 33).

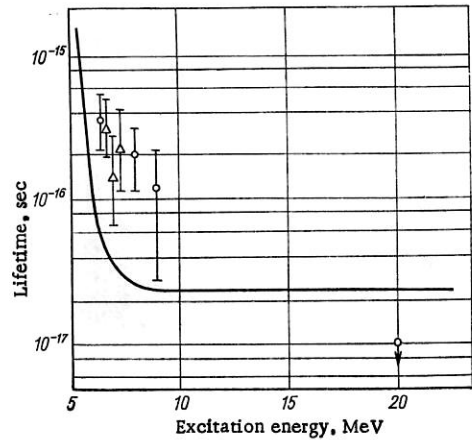


Fig. 15. Dependence of the lifetime of the compound nucleus on the excitation energy (from the data in Table 3). Circles) Data of refs. 33, 39; triangles) data of ref. 40; curve) calculated from a constant-temperature model with the parameters $T = 0.6$ MeV, $B_f^* = 5.8$ MeV, $B_n^* = 5.75$ MeV, and $r_0 = 1.25 \cdot 10^{-13}$ cm.

sults were found for other neutron energies. Table 3 shows all the available experimental results on the lifetime of the compound nuclei formed by irradiating uranium with light particles. Since these compound nuclei do not differ appreciably in nucleon composition, all these lifetimes can be compared. Figure 15 shows the lifetime of the compound nucleus as a function of the excitation energy found from the data in Table 3. We see a regular decrease in the lifetime with increasing excitation energy which is qualitatively consistent with the statistical model. These results will be discussed in more detail in the following section.

We turn now to experiments involving fission of ^{181}Ta and ^{186}W by accelerated heavy ions of ^{11}B , ^{12}C , ^{16}O , ^{22}Ne , and ^{31}P . The compound nuclei formed in these reactions have a high excitation energy of ≈ 60 MeV even when the energy of the incident particles is equal to the Coulomb barrier. We might therefore expect the lifetimes to be much shorter than 10^{-16} sec. On the other hand, the velocity acquired by the compound nuclei in reactions induced by heavy ions is much higher than the velocity of

TABLE 3. Measured Lifetimes of Compound Nuclei in the Fission of Uranium by Neutrons, Protons, and α Particles

Reaction	Particle energy, MeV	Compound nucleus	Excitation energy, MeV	Velocity of compound nucleus, 10^7 cm/sec	$\Delta\chi$	$\tau, 10^{-16}$ sec	Reference
$^{238}\text{U}(n, f)$	1.7	^{239}U	6.5	0.76	0.20 ± 0.11	(3.5 ± 1.0)	[33]
$^{238}\text{U}(n, f)$	3.3	^{239}U	8.1	1.06	0.13 ± 0.10	(2.0 ± 0.8)	[28, 33]
$^{238}\text{U}(\alpha, f)$	25	^{242}Pu	20	5.90	$< 0.01 \pm 0.06$	< 0.1	[25]
$^{238}\text{U}(p, n, f)$	10	^{238}Np	~ 7	1.90	0.066 ± 0.021	(1.4 ± 0.8)	[27]
$^{238}\text{U}(n, f)$	1.8	^{239}U	6.6	0.76	0.19 ± 0.10	(3.2 ± 1.0)	[40]
$^{238}\text{U}(n, f)$	2.5	^{239}U	7.3	0.91	0.13 ± 0.10	(2.3 ± 1.6)	[40]
$^{238}\text{U}(n, f)$	4.2	^{239}U	9.0	1.15	0.06 ± 0.05	(1.2 ± 1.0)	[39]

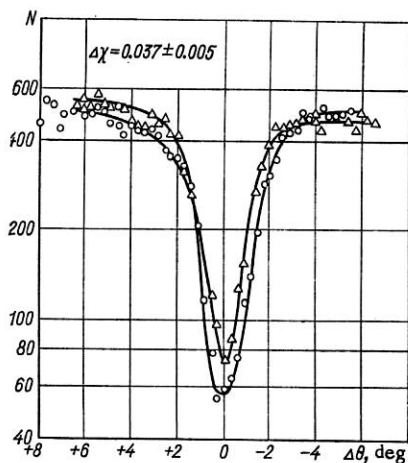


Fig. 16. Angular distribution of fission fragments near tungsten $\langle 111 \rangle$ axes oriented at angles of 90° (triangles) and 160° (circles) with respect to the beam of 174-MeV ^{22}Ne ions.³⁰

the compound nuclei in the reactions discussed above, so the lifetime range which can be measured is shifted toward shorter values (Fig. 2). It was thus necessary in the earliest heavy-ion experiments to determine whether conditions could be arranged in which the actual lifetime of the compound nucleus fell within the lifetime range measurable by the blocking effect.

In the first heavy-ion experiments dips were detected in the angular distributions of fission fragment produced by irradiating a tungsten crystal of natural isotopic composition with accelerated ^{22}Ne ions.²⁹ The angular width of the dips turned out to be near the theoretical predictions in this case. The dip depth was $\chi = 0.25$, showing the crystal to be of good quality and showing that radiation damage to the crystal by the heavy-ion beam did not significantly change the blocking pattern over an exposure time of about 10 h. This χ value revealed a lifetime of $\tau \leq 8 \cdot 10^{-18}$ sec for the compound nucleus in this reaction for an excitation energy of 117 MeV. In a further study of the reaction $W(^{22}\text{Ne}, f)$ (refs. 30, 35) a difference was found between the dip depths corresponding to two identical $\langle 111 \rangle$ axes of a tungsten crystal making angles of 90° and 160° with respect to the ion beam. Figure 16 shows

TABLE 4. Lifetimes Measured in Fission of Tungsten Nuclei by Accelerated Heavy Ions

Direction	E_1^{max} , MeV	E_c^* , MeV	v_c , 10^8 cm/sec	$\Delta\chi$	τ , 10^{-18} sec
$W(^{22}\text{Ne}, f)$	174	116	4.13	0.040 ± 0.003	2.54
$W(^{22}\text{Ne}, f)$	146	91	3.77	0.051 ± 0.008	3.27
$W(^{22}\text{Ne}, f)$	116	65	3.35	0.070 ± 0.004	4.02
$W(^{20}\text{Ne}, f)$	192	132	4.22	0.041 ± 0.008	2.42
$W(^{16}\text{O}, f)$	137	99	3.22	0.012 ± 0.015	≤ 2.11
$W(^{16}\text{O}, f)$	97	62	2.69	0.091 ± 0.015	5.64
$W(^{12}\text{C}, f)$	80	62	2.22	0.082 ± 0.010	6.30

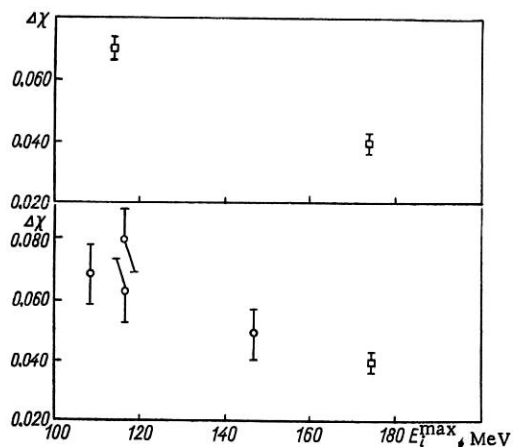


Fig. 17. Dependence of the quantity $\Delta\chi = \chi(90^\circ) - \chi(160^\circ)$ on the energy of the bombarding particles for the reaction $W(^{22}\text{Ne}, f)$ (ref. 30). The values of $\Delta\chi$ shown at the top of the figure are averages over several experiments.

the angular distributions of fragments near these axes for the case of ^{22}Ne ions having an energy of 174 MeV. Figure 17 shows the energy dependence of the quantity $\Delta\chi = \chi(90^\circ) - \chi(160^\circ)$ as the energy of the ^{22}Ne ions is varied from 108 to 174 MeV. This dependence is strong additional evidence that the observed difference between dip depths is related to the displacement of the fissioning nucleus from the lattice site. Table 4 shows the results of an experimental study³² of fission of tungsten nuclei induced by ^{12}C , ^{16}O , and ^{22}Ne ions. The lifetimes were calculated from Eq. (10) with a cutoff radius of $r_c = 0.4$ Å. Figure 18 shows the quantity $\Delta\chi = \chi(90^\circ) - \chi(160^\circ)$ calculated from Eq. (10) as a function of the product $v\tau$ for various cutoff radii r_c . The following basic conclusions can be drawn from these results: The lifetimes of highly excited compound nuclei in the reactions $W(^{12}\text{C}, f)$, $W(^{16}\text{O}, f)$, and $W(^{22}\text{Ne}, f)$ are on the order of 10^{-18} sec; the energy dependences of the lifetimes for these reactions differ markedly.

The target in these experiments was a tungsten single crystal of natural isotopic composition. The mass number and excitation energy of the fissioning compound

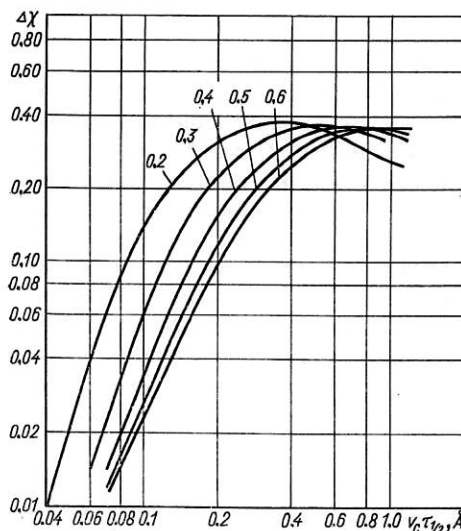


Fig. 18. Calculated dependence of the quantity $\Delta\chi = \chi(90^\circ) - \chi(160^\circ)$ on the product $v\tau$ (ref. 30).

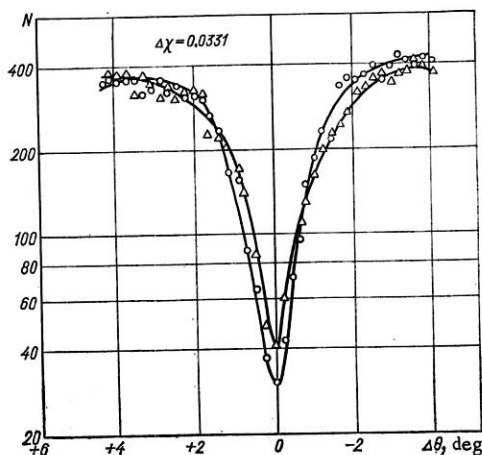


Fig. 19. Dependence of the number of fission-fragment tracks per unit area of the dielectric detector on the angular distance from one of the two crystallographic $\langle 111 \rangle$ axes. Triangles) $\langle 111 \rangle$ axis making an angle of 90° with respect to the beam; circles) $\langle 111 \rangle$ axis making an angle of 160° with respect to the beam. The reaction is $^{186}\text{W} (^{31}\text{P}, f)$; the ion energy is 195 MeV (ref. 36).

nuclei formed during irradiation of the target by the various particles were spread over certain ranges. In an effort to clearly fix the parameters of the compound nucleus, further experiments were carried out³⁶ with tantalum crystals of natural isotopic composition (99.99% ^{181}Ta) and tungsten single crystals enriched with ^{186}W (90.5% ^{186}W). The bombarding particles in these experiments were heavy ions accelerated by the U-300 cyclotron of the Nuclear Reactions Laboratory of the Joint Institute for Nuclear Research: 87-MeV ^{11}B ions; 80-MeV ^{12}C ions; 137-MeV ^{16}O ions; 174-MeV ^{22}Ne ions, and 195-MeV ^{31}P ions. A beam of 108-MeV ^{12}C ions extracted from the U-200 cyclotron was also used. In all the reactions the measurements were carried out at the maximum beam energy and at a beam energy reduced by retarding foils to a value near the Coulomb barrier for the interacting nuclei.

The fission-fragment detectors used in the experiments with ^{31}P ions were fused quartz detectors, which did not detect elastically scattered phosphorus ions. The silicate-glass detectors used to study reactions with lighter bombarding particles reliably identified the elastically scattered ions. Figures 19 and 20 show the results found in a microscopic study of the detectors (of the diametral cross sections of the axial blocking patterns) for the case of the $^{186}\text{W} (^{31}\text{P}, f)$ reaction with ion energies of 195 and 155 MeV (ref. 36). Similar diagrams were found for all the other reactions studied. We see that for all the reactions the dips corresponding to axes making an angle of 160° with respect to the beam are deeper than those for an angle of 90° . The depth difference $\Delta\chi = \chi(90^\circ) - \chi(160^\circ)$ varies with the energy of the bombarding particle and from reaction to reaction, reflecting the changes in the lifetime of the compound nucleus as a function of the nature of the particle and its energy. Figures 19 and 20 show typical results.

The dip depth $\chi(90^\circ)$ and $\chi(160^\circ)$ and their difference $\Delta\chi$ are determined accurately in the following manner: The tracks are counted in the field of view of the microscope at many positions along the periphery of the axial dip, and the average track density outside the dip (A) is

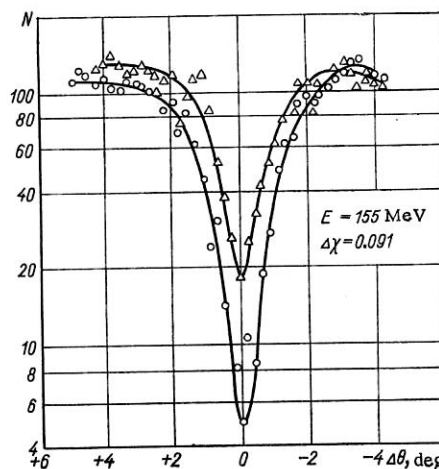


Fig. 20. The same as in Fig. 19, for the reaction $^{186}\text{W} (^{31}\text{P}, f)$ for ^{31}P ions having an energy of 155 MeV (ref. 36). Triangles) 90° ; circles) 160° .

determined with a statistical error $< 1\%$. Since the track density at the center of the dip is much lower than that at the periphery, a region consisting of 100 fields of view near the intensity minimum was scanned. A square formed by nine of 16 fields of view was chosen for which the sum of the number of tracks was minimal (in comparison with the sums for all other such squares). The average number of tracks per field of view in the square is the quantity B; when this quantity is divided by A, we find the dip depth $\chi = B/A$ with a total relative error of $\delta\chi/\chi = \delta A/A + \delta B/B$. The relative error $\delta\chi/\chi$ was usually 3–5%. For the difference $\chi(90^\circ) - \chi(160^\circ) = \Delta\chi$ the statistical error did not exceed 30%.

The mean lifetimes of the compound nuclei were determined from the measured values of $\Delta\chi$. Table 5 shows the reactions studied and the corresponding lifetimes found for two values of the cutoff radius r_c of the atomic potential. Here a few words are in order about the method for choosing r_c and the effect of this choice on the lifetime found. The usual assumption is $r_c \approx 0.4 \text{ \AA}$ was used to obtain agreement between the results found by the numerical simulation on the computer and those calculated through the use of the cutoff radius. It is interesting to examine the sensitivity of the lifetimes to the values of r_c . Table 5 shows results found for two values of r_c (ref. 36). We see that as r_c is changed from 0.2 to 0.4 \AA , the

TABLE 5. Experimental Results Found with ^{186}W and ^{181}Ta Crystals (ref. 36)

Reaction	$E_{\text{ion}}, \text{ MeV}$	$E^*, \text{ MeV}$	$\Delta\chi$	$\tau_{\text{expt}}, 10^{-10} \text{ sec}$		$\tau_{\text{theo}}, 10^{-10} \text{ sec}$	
				$r_c = 0.4 \text{ \AA}$	$r_c = 0.2 \text{ \AA}$	$a_n = a_c = A/8$	$a_n = a_c = A/4$
$^{186}\text{W}(^{11}\text{B}, f)$	87	80	0.096 ± 0.014	69	38	0.79	16
$^{186}\text{W}(^{12}\text{C}, f)$	80	64	0.087 ± 0.015	67	37	1.1	22
$^{186}\text{W}(^{13}\text{C}, f)$	108	89	0.007 ± 0.015	≤ 19	≤ 11	0.29	4.2
$^{181}\text{Ta}(^{16}\text{O}, f)$	96	63	0.104 ± 0.047	60	32	3.7	130
$^{181}\text{Ta}(^{16}\text{O}, f)$	137	101	0.004 ± 0.035	≤ 33	≤ 18	0.45	8.1
$^{186}\text{W}(^{16}\text{O}, f)$	97	67	0.083 ± 0.015	52	29	1.2	26
$^{186}\text{W}(^{16}\text{O}, f)$	137	103	0.015 ± 0.008	22	12	0.22	3.1
$^{181}\text{Ta}(^{22}\text{Ne}, f)$	116	69	0.044 ± 0.030	33	19	3.3	110
$^{181}\text{Ta}(^{22}\text{Ne}, f)$	174	120	0.081 ± 0.030	37	21	0.35	4.4
$^{186}\text{W}(^{22}\text{Ne}, f)$	116	68	0.080 ± 0.015	42	23	1.5	36
$^{186}\text{W}(^{22}\text{Ne}, f)$	174	119	0.046 ± 0.015	27	15	0.14	2.0
$^{181}\text{Ta}(^{31}\text{P}, f)$	155	60	0.023 ± 0.034	≤ 27	≤ 15	9.3	430
$^{181}\text{Ta}(^{31}\text{P}, f)$	195	94	0.047 ± 0.030	22	12	0.81	17
$^{186}\text{W}(^{31}\text{P}, f)$	155	59	0.091 ± 0.008	33	18	1.8	43
$^{186}\text{W}(^{31}\text{P}, f)$	195	92	0.033 ± 0.009	20	11	0.27	3.6

the absolute lifetime changes by a factor of about 2, but there is only a slight effect on the relative lifetimes for different reactions and different excitation energies. To establish empirical dependences of τ on the atomic number of the compound nucleus and its excitation energy it is desirable to analyze the data for some selected cutoff radius, e.g., $r_c = 0.4 \text{ \AA}$; the results of such an analysis are shown in Fig. 21. We see that for an excitation energy of about 60 MeV an increase in Z is accompanied by a monotonic decrease in the lifetime. From the dependence of the lifetime on the excitation energy we see that the rate of change of the lifetime, $\Delta\tau/\Delta E^*$, decreases with increasing atomic number of the compound nucleus. This behavior is discussed in the following section.

RESULTS OF BLOCKING-EFFECT MEASUREMENTS OF NUCLEAR REACTION TIMES

The results found for nuclear reaction times in blocking-effect experiments are of considerable methodological interest and are also of interest from a general physical point of view. As was mentioned above, for methodological purposes it is very important to compare the lifetimes found for isolated resonances found by the blocking method with results found in "traditional" nuclear experiments, namely from level widths.

As we see from Table 1, the resonance (p, α) reactions show that the results of the two types are approximately equal. Furthermore, there is a good agreement among the results obtained by different groups of investigators for the lifetime of the arsenic nuclei which are the compound nuclei involved in the inelastic scattering of protons by germanium (Table 2). This agreement is even more interesting in that the finite lifetime is observed to affect different elements of the blocking pattern (for both axial^{31,41} and planar²⁶ patterns). Different parameters have been used as the quantitative characteristic (the particle intensity at the center of the dip⁴¹ and the total number of particles ejected as a result of Coulomb collisions with the axis³¹ or plane²⁶). Different methods have also been used to convert from the observed effect to the lifetime of the compound nucleus [the method involving a cutoff radius for the atomic potential,⁴¹ the analytic method²⁶ corresponding to Eqs. (14)–(16), and

numerical simulation on a computer³¹]. A result of considerable physical interest found in the study of (p, p') reactions in germanium isotopes is the order of magnitude itself of the lifetime involved ($\sim 10^{-17}$ sec). The lifetimes measured for the compound nuclei ^{71}As and ^{73}As have been used to find the level-density parameters,³¹ which have turned out to be very nearly equal to those calculated on the basis of the familiar semiempirical equation.⁴⁹

Also of considerable interest is the attempt to study the influence of isobaric analog resonances on the mean lifetime of the compound nucleus formed in the inelastic scattering of protons by germanium.⁴¹ Experiments with very thin crystals (1.5μ), which provide an energy resolution no worse than 30 keV, have revealed a decrease of 20–25% in this mean lifetime in the case in which the energy of the incident protons corresponds to the analog resonance in the excitation function. This study also revealed that the spin of the product nucleus affects the lifetime of the compound nucleus in the $\text{Ge}(p, p')$ reaction; this effect may be attributable to angular-momentum selection of the excited levels of the compound nucleus.

We turn now to the results obtained in measurements of the lifetimes of fissioning compound nuclei. These results can be meaningfully discussed on the basis of the results obtained in the earlier analysis of the empirical behavior of the width ratio Γ_f/Γ_n as a function of the atomic number and excitation energy of the nuclei. At present we can tentatively classify all nuclei into two groups for a discussion of the ratio Γ_f/Γ_n : 1) nuclei with $Z < 85$ which undergo fission relatively weakly; 2) nuclei with $Z > 90$ which are highly fissile. The boundary between these two groups is of course arbitrary and may depend on neutron enrichment of the nuclei and on the excitation energy. The principle difference between these two groups is apparently the circumstance that with $Z > 90$ the fission barrier is on the order of or lower than the neutron binding energy, while the weakly fissile nuclei have a high fission barrier, far above the neutron binding energy. Significantly different compound-nucleus models are used to describe the ratio Γ_f/Γ_n for these two groups of nuclei: the Fermi-gas model for the first group, and the constant-temperature model for the second. At present the physical reasons for this difference in behavior are not understood.

In the Fermi-gas model the level density of the compound nucleus is given as a function of the excitation energy by

$$\rho(E) = \text{const} \exp(2\sqrt{aE}). \quad (21)$$

Approximate equations have been obtained⁵⁰ in the Fermi-gas model for Γ_n , Γ_f , and Γ_n/Γ_f on the basis of a statistical analysis of neutron evaporation and fission, first carried out in refs. 51 and 52:

$$\Gamma_n = \frac{A^{2/3}(E - B_n)}{a_n \pi K_0 \exp[2(a_n E)^{1/2}]} \exp[2a_n^{1/2}(E - B_n)^{1/2}]; \quad (22)$$

$$\Gamma_f = \frac{2a_f^{1/2}(E - B_f)^{1/2} - 1}{4a_f \pi \exp[2(a_f E)^{1/2}]} \exp[2a_f^{1/2}(E - B_f)^{1/2}]; \quad (23)$$

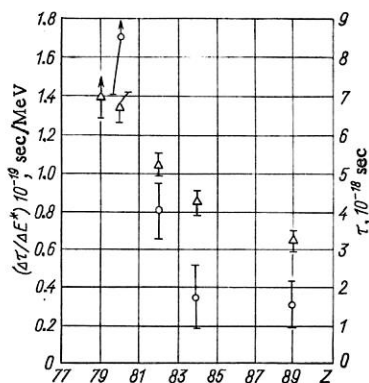


Fig. 21. Lifetime of the compound nucleus (τ) at an excitation energy of 60 MeV and rate of change of τ with increasing excitation energy ($\Delta\tau/\Delta E^*$) as functions of the atomic number Z of the compound nucleus. Triangles) τ ; circles) $\Delta\tau/\Delta E^*$.

$$\Gamma_n/\Gamma_f = \frac{4A^{2/3}a_f(E-B_n)}{K_0a_n[2a_f^{1/2}(E-B_f)^{1/2}-1]} \times \exp\{2a_n^{1/2}(E-B_n)^{1/2}-2a_f^{1/2}(E-B_f)^{1/2}\}, \quad (24)$$

where $K_0 = \hbar^2/(2mr_0^2)$; and a_c , a_n , and a_f are, respectively, the level-density parameters of the original compound nucleus, the nucleus left after the neutron evaporation, and the compound nucleus at the saddle point. Parameters a_c and a_n are usually assumed equal for heavy nuclei.

For weakly fissile nuclei it has been established experimentally that Γ_f/Γ_n increases with increasing energy, i.e., Γ_f increases more rapidly than Γ_n , and at high excitation energies the Γ_f value exceeds Γ_n ($\Gamma_f/\Gamma_n > 1$), despite the inequality $B_f > B_n$. This behavior of Γ_f/Γ_n can be achieved with the Fermi-gas model only if the assumption $a_f > a_n$ is used. Quantitative analysis of the experimental data for Γ_f/Γ_n for the fission of rare-earth elements and tungsten by heavy nuclei has revealed a satisfactory agreement between experiment and theory (with the values $a_f = A/8$ and $a_n = A/10$) for excitation energies not exceeding 70–80 MeV (ref. 53). At higher excitation energies there is a systematic discrepancy: The theoretical values of Γ_f/Γ_n continue to increase rapidly, while the experimental values display a tendency toward saturation. This discrepancy can be eliminated by assuming that a_n increases with increasing excitation energy, approaching a_f , which remains constant. We also note that, according to Eq. (24), the ratio Γ_f/Γ_n is sensitive primarily to the ratio a_f/a_n and not to the magnitude of one or the other of these parameters, so an equally satisfactory description of Γ_f/Γ_n can be obtained even with other absolute value of the level-density parameters.

Let us compare the predictions of the Fermi-gas model regarding the width $\Gamma = \Gamma_f + \Gamma_n$ with the experimental values of the lifetimes of highly excited nuclei produced in reactions induced by heavy ions. Calculation on the basis of (23) with the values $a_f = A/8$ and $a_n = A/10$ yields lifetimes ($\tau = \hbar/\Gamma$) on the order of 10^{-19} – 10^{-20} sec for all the reactions which have been studied, while the experimental values are on the order of 10^{-18} sec. This discrepancy can be eliminated by choosing level-density parameters in the range $A/4$ – $A/5$. Table 5 shows the calculated $\tau_n = \hbar/\Gamma_n$ values. As was mentioned above, the agreement between the theoretical and experimental Γ_f/Γ_n values is retained. However, the energy dependence of the lifetime of the compound nucleus is also important. According to Eqs. (22) and (23), the quantities Γ_n , Γ_f , and thus Γ are rapidly increasing functions of E^* in the excitation-energy range of interest. Experimentally, on the other hand, we find the lifetime to fall off relatively slightly with increasing excitation energy for most of the reactions. Only for the lightest of the compound nuclei studied, those found in the reactions $^{186}\text{W} (^{12}\text{C}, f)$ and $^{186}\text{W} (^{16}\text{O}, f)$, does the lifetime fall off sufficiently rapidly (Table 5 and Fig. 21). We can thus achieve a qualitative agreement between experiment and the Fermi-gas model only with compound nuclei in the range $79 < Z < 82$. For the compound nucleus ^{208}Po the lifetime falls off by a factor of only 1.5 as the excitation energy increases from 68 to 119 MeV.

For the heavier nuclei we find an analogous situation. This weak dependence of the lifetime on the excitation en-

ergy corresponds closely to the predictions of the constant-temperature model, to which we now turn.

In the constant-temperature model⁵⁰ the level density of the compound nucleus is given by

$$\rho(E) = \text{const} \exp(E/T). \quad (25)$$

Using the equations of refs. 51 and 52, we can then easily find

$$\Gamma_n = \frac{A^{2/3}T^2}{\pi K_0} \exp(-E/T) \{\exp[(E-B_n)/T] - (E-B_n)/T - 1\}; \quad (26)$$

$$\Gamma_f = (T/2\pi) \exp(-E/T) \{\exp[(E-B_f)/T] - 1\}. \quad (27)$$

For $E-B_n > 4T$ and $E-B_f > 3T$ these equations can be replaced (with an error of less than 1%) by the approximations

$$\Gamma_n = (A^{2/3}T^2/\pi K_0) \exp(-B_n/T); \quad (28)$$

$$\Gamma_f = (T/2\pi) \exp(-B_f/T); \quad (29)$$

$$\Gamma_f/\Gamma_n = (K_0/2A^{2/3}T) \exp[-(B_f-B_n)/T]. \quad (30)$$

It is easy to see that according to the constant-temperature model the values of Γ_n and Γ_f increase rapidly with increasing excitation energy only near B_n and B_f , respectively, and they rapidly assume the constant values given by Eqs. (28) and (29). The ratio Γ_f/Γ_n behaves in a similar manner. The constant-temperature model also agrees better with experiment in the description of the Γ_f/Γ_n behavior for highly fissile nuclei, for which an extremely slight change in Γ_f/Γ_n has been found experimentally for a large change in the excitation energy. On the other hand, this model does not describe Γ_f/Γ_n well in the range $Z < 85$. There is no change we can make in the single parameter T which will reproduce the observed monotonic increase in Γ_f/Γ_n over a broad range of excitation energies or which will yield a ratio Γ_f/Γ_n approximately unity for nuclei having $B_f \gg B_n$. Nevertheless, the fact that the lifetimes measured in heavy-ion-induced reactions for compound nuclei with $Z > 84$ depend weakly on the excitation energy and have values on the same order of magnitude as those which can be found in the constant-temperature model with $T \approx 1$ MeV, is a strong argument in favor of the use of this model for describing highly excited nuclei with $Z > 84$. Further evidence in favor of this argument comes from the measured⁵⁴ cross sections for the reaction $^{164}\text{Dy} (^{40}\text{Ar}, xn) ^{204-x}\text{Po}$, which are satisfactorily described by a calculation in which Γ_f/Γ_n is assumed independent of the energy.

We turn now to a comparison of the predictions of the constant-temperature model with the experimental lifetimes of the compound nuclei formed in the interaction of ^{238}U nuclei with neutrons, protons, and α particles (Table 3). In Fig. 15 the lifetimes found for the various reactions are shown as a function of the excitation energy without regard for the differences among the Z and A values of the nuclei. This figure also shows the calculated dependence of the lifetime on the excitation energy of the ^{238}U nucleus for the parameter value $T = 0.6$ MeV. We see that there is a good qualitative agreement between theory and experiment.

We can draw the following conclusions from this dis-

cussion. In the range of highly fissile nuclei ($Z \approx 92$) the constant-temperature model gives a satisfactory description of not only the ratio Γ_f/Γ_n but also the absolute values of the widths. This model is probably also applicable for the decay widths of highly excited nuclei with $Z > 84$. For heavier nuclei the Fermi-gas model gives a better description of Γ_f/Γ_n and of the lifetimes of the excited nuclei.

It is somewhat surprising to find such a strong change in the level-density function (i.e., the transition from the Fermi-gas model to the constant-temperature model) as a function of the atomic number of the nucleus. It may be that a more profound theoretical analysis is required of the theoretical values of the ratio Γ_f/Γ_n and the lifetimes of compound nuclei in the range $75 < Z < 90$. It would apparently be worthwhile to attempt to improve the constant-temperature model to make it applicable for weakly fissile nuclei. The basic difficulty which arises here, as mentioned above, lies in the fact that the Γ_f/Γ_n value cannot be increased to a value near unity as the excitation energy is increased. This difficulty might be overcome by assuming that the highly deformed nucleus at the saddle point is characterized by a completely different temperature parameter than at a deformation near equilibrium. Using the general expression⁵² for the fission width we then find

$$\Gamma_f = (T_f/2\pi) \exp(-E/T_c) \{ \exp[(E - B_f)/T_f] - 1 \} \quad (31)$$

or, in the high-energy limit,

$$\Gamma_f = (T_f/2\pi) \exp \{-E(1/T_c - 1/T_f) - B_f/T_f\}, \quad (32)$$

where T_f is the temperature parameter for the nucleus at the saddle point, and T_c is the temperature parameter for the equilibrium deformation.

When a parameter value $T_f < T_c$ is used, this equation can yield large values of Γ_f , even for nuclei having a high barrier B_f . Another possible way to find a common description of the decay widths of highly and weakly fissile nuclei would be to seek a universal level-density function as a function of the excitation energy. Yet a third possibility would be to use the Fermi-gas model with level-density parameters dependent on the excitation energy, deformation, and shell structure of the nucleus. Attempts are currently being made^{55,56} to calculate these dependences for level-density parameters in a microscopic approach.

In conclusion we can point out the most urgent problems lying ahead in the development of the blocking method for measuring the lifetimes of excited compound nuclei. The most important problem is apparently that of making a detailed study to determine which parameter of the blocking pattern is most sensitive to the displacement of the compound nucleus but which is also sufficiently insensitive to the effects of various interfering factors. The success of this study will govern both the future usefulness of the method, i.e., the lower limit on the lifetimes measurable by this method, and the accuracy of the results. Establishment of a logical basis for the method requires a solution of the problem of determining the mean lifetime of the compound nucleus from the magnitude of the observed effect under conditions as real as possible.

- ¹T. Ericson, Phys. Rev. Lett., **5**, 430 (1960).
- ²T. Ericson, Adv. Phys., **9**, 425 (1960).
- ³T. Ericson, Ann. Phys. (New York), **23**, 390 (1963).
- ⁴T. Ericson, Phys. Lett., **4**, 258 (1963).
- ⁵T. Ericson and T. Mayer-Kuckuk, Annual Reviews of Nuclear Science, Vol. 16 (1966).
- ⁶E. L. Feinberg, in: Proceedings of the Symposium on Problems in Nuclear Physics [in Russian], Vol. 2, Tbilisi (1967), p. 389.
- ⁷P. Fessenden, W. Gibbs, and R. Leachman, Phys. Rev. Lett., **15**, 796 (1965).
- ⁸P. Fessenden, W. Gibbs, and R. Leachman, Phys. Rev., **C3**, 807 (1971).
- ⁹M. T. Robinson and O. S. Oen, Phys. Rev., **132**, 2385 (1963).
- ¹⁰J. Lindhard, Mat. Fys. Medd. Dan. Vid. Selsk., **34**, No. 14 (1965).
- ¹¹B. Domeij and K. Björqvist, Phys. Lett., **14**, 127 (1965).
- ¹²A. F. Tulinov, Dokl. Akad. Nauk SSSR, **162**, 546 (1965) [Sov. Phys. - Dokl., **10**, 463 (1965)].
- ¹³D. S. Gemmell and R. E. Holland, Phys. Rev. Lett., **14**, 945 (1965).
- ¹⁴A. F. Tulinov et al., ZhETF Pis. Red., **2**, 48 (1965) [JETP Lett., **2**, 30 (1965)]; A. F. Tulinov, V. S. Kulikauskas, and M. M. Malov, Phys. Lett., **18**, 304 (1965).
- ¹⁵P. Lervig, J. Lindhard, and V. Nielsen, Nucl. Phys., **A96**, 481 (1967).
- ¹⁶Yu. M. Kagan and Yu. V. Kononets, Zh. Éksp. Teor. Fiz., **58**, 226 (1970) [Sov. Phys. - JETP, **31**, 124 (1970)].
- ¹⁷G. Molière, Z. für Naturforschung, **2a**, 133 (1947).
- ¹⁸V. A. Ryabov, Dissertation [in Russian] (1969).
- ¹⁹J. U. Andersen, Mat. Fys. Medd. Dan. Vid. Selsk., **36**, No. 7 (1967).
- ²⁰L. C. Feldman, Dissertation (1967).
- ²¹J. H. Barrett, Phys. Rev. B, **3**, 1527 (1971).
- ²²A. F. Tulinov, Vestn. MGU, Ser. Fiz., **5**, 88 (1967).
- ²³F. Brown, D. A. Marsden, and R. D. Werner, Phys. Rev. Lett., **20**, 1449 (1968).
- ²⁴Yu. V. Melikov et al., Zh. Eksp. Teor. Fiz., **55**, 1690 (1968) [Sov. Phys. - JETP, **28**, 888 (1969)].
- ²⁵Yu. V. Melikov, Yu. D. Ostavnov, and A. F. Tulinov, Zh. Eksp. Teor. Fiz., **56**, 1803 (1969) [Sov. Phys. - JETP, **29**, 968 (1969)].
- ²⁶M. Maruyama et al., Phys. Lett. B, **29**, 414 (1969); Nucl. Phys. A, **145**, 581 (1970).
- ²⁷W. M. Gibson and K. O. Nielsen, Phys. Rev. Lett., **24**, 114 (1969).
- ²⁸Yu. V. Melikov, Yu. D. Ostavnov, and A. F. Tulinov, Yad. Fiz., **12**, 50 (1970) [Sov. J. Nucl. Phys., **12**, 27 (1971)].
- ²⁹S. A. Karamyan et al., Yad. Fiz., **13**, 944 (1970).
- ³⁰S. A. Karamyan, F. Normuratov, and Yu. Ts. Oganessian, Yad. Fiz., **14**, 499 (1971) [Sov. J. Nucl. Phys., **14**, 279 (1972)].
- ³¹G. Clark et al., Nucl. Phys. A, **173**, 73 (1971).
- ³²S. A. Karamyan, F. Normuratov, and Yu. Ts. Oganessian, in: Collected Works of the Joint Institute for Nuclear Research [in Russian], D7-5769, Dubna (1971).
- ³³Yu. V. Melikov et al., Nucl. Phys. A, **180**, 241 (1972).
- ³⁴K. Komaki et al., Phys. Lett. B, **38**, 218 (1972).
- ³⁵V. V. Kamanin et al., Yad. Fiz., **16**, 252 (1972) [Sov. J. Nucl. Phys., **16**, 140 (1973)].
- ³⁶V. V. Kamanin et al., Yad. Fiz., **16**, 447 (1972) [Sov. J. Nucl. Phys., **16**, 249 (1973)].
- ³⁷Yu. V. Melikov et al., Report to the Fourth All-Union Conference on the Physics of the Interaction of Charged Particles with Single Crystals, Moscow, 1972.
- ³⁸O. V. Bormot et al., Report to the Fourth All-Union Conference on the Physics of the Interaction of Charged Particles with Single Crystals, Moscow, 1972.
- ³⁹P. E. Vorotnikov et al., Report to the Fourth All-Union Conference on the Physics of the Interaction of Charged Particles with Single Crystals, Moscow, 1972.
- ⁴⁰K. O. Nielsen, Report to the Fourth All-Union Conference on the Physics of the Interaction of Charged Particles with Single Crystals, Moscow, 1972.
- ⁴¹W. M. Gibson, Report to the Fourth All-Union Conference on the Physics of the Interaction of Charged Particles with Single Crystals, Moscow, 1972.
- ⁴²G. P. Pokhil and A. F. Tulinov, Report to the Fourth All-Union Conference on the Physics of the Interaction of Charged with Single Crystals, Moscow, 1972.
- ⁴³K. Komaki and F. Fujimoto, Phys. Lett. A, **29**, 544 (1969); Phys. Status Solidi (a), **2**, 875 (1970).
- ⁴⁴L. Massa, Lett. Nuovo Cimento, **III**, No. 6, 186 (1970).
- ⁴⁵P. Sona, Nuovo Cimento A, **66**, No. 4, 663 (1970).

- ⁴⁶J. H. Barrett, *Bull. Amer. Phys. Soc.*, **14**, 372 (1969).
- ⁴⁷A. I. Baz', Ya. B. Zel'dovich, and A. M. Perelomov, *Scattering, Reactions, and Decay in Nonrelativistic Quantum Mechanics* [in Russian], Nauka, Moscow (1966).
- ⁴⁸F. Malaguti, A. Uguzzoni, and E. Verondini, *Lett. Nuovo Cimento*, **2**, No. 13, 629 (1971).
- ⁴⁹A. Gilbert and A. G. W. Cameron, *Can. J. Phys.*, **43**, 1446 (1965).
- ⁵⁰J. R. Hulzenga and R. Vandenbosh, in: *Nuclear Reactions*, Vol. II, ed. P. M. Endt and P. B. Smith, Wiley, New York (1962).
- ⁵¹V. F. Weisskopf, *Phys. Rev.*, **52**, 295 (1937).
- ⁵²N. Bohr and J. A. Wheeler, *Phys. Rev.*, **56**, 426 (1939).
- ⁵³T. Sikkeland, *Phys. Rev. B*, **135**, 669 (1964).
- ⁵⁴T. Sikkeland et al., *Phys. Rev. C*, **1**, 1564 (1970).
- ⁵⁵A. V. Ignatyuk, V. S. Stavinskii, and Yu. N. Shubin, *Yad. Fiz.*, **11**, 1012 (1970).
- ⁵⁶A. V. Ignatyuk and V. S. Stavinskii, *Yad. Fiz.*, **11**, 1213 (1970).